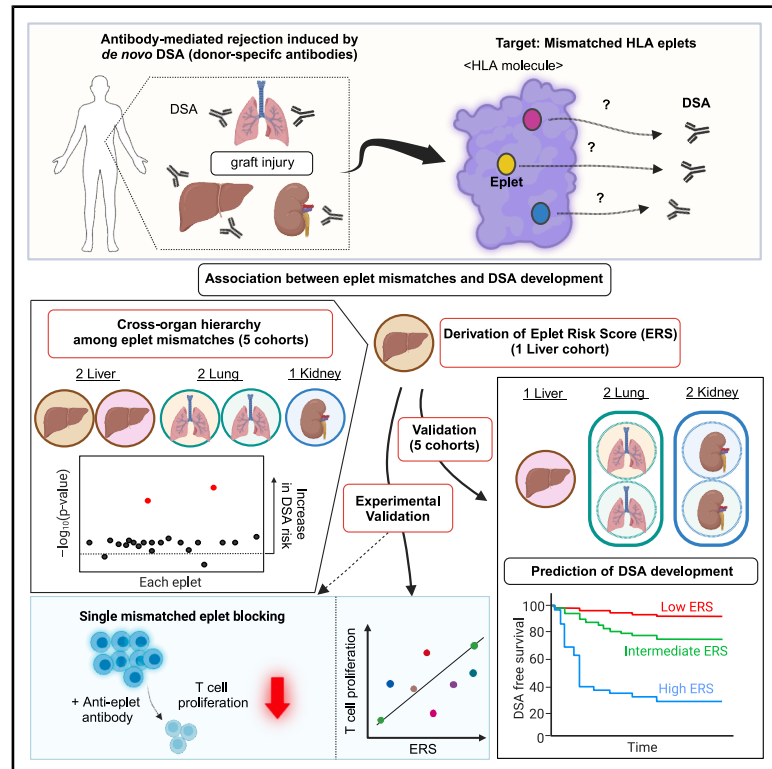


Cross-organ hierarchy of HLA molecular mismatches in donor-specific antibody development in solid organ transplantations

Graphical abstract



Authors

Masaaki Hirata, Kazuto Tsukita, Takero Shindo, ..., Takashi Kobayashi, Hiroshi Date, Etsuro Hatano

Correspondence

takeros@kuhp.kyoto-u.ac.jp

In brief

Hirata et al. reveal a cross-organ hierarchy among HLA eplet mismatches driving DSA risk in solid organ transplantations. They introduce an eplet risk score (ERS) that captures this hierarchy and correlates with $CD4^+$ T cell proliferation *in vitro*, providing a tool for accurate prediction of DSA development across organ types.

Highlights

- Eplet-wide analyses reveal a hierarchy among HLA eplet mismatches driving DSA risk
- This hierarchy is conserved across various solid organ transplantations
- Eplet risk score (ERS) captures this hierarchy, accurately predicting DSA development
- ERS correlates with $CD4^+$ T cell proliferation in mixed lymphocyte reaction



Article

Cross-organ hierarchy of HLA molecular mismatches in donor-specific antibody development in solid organ transplantations

Masaaki Hirata,^{1,14} Kazuto Tsukita,^{2,3,4,14} Takero Shindo,^{5,6,15,*} Shintaro Yagi,^{1,7} Takashi Ito,¹ Satona Tanaka,⁸ Ryo Fujimoto,⁸ Hidenao Kayawake,⁸ Kenji Nakamura,⁹ Nobuhiro Fujiyama,¹⁰ Mitsuru Saito,¹¹ Kimiko Yurugi,¹² Rie Hishida,¹² Arisa Kato,⁵ Atsushi Kawaguchi,¹³ Tomonori Habuchi,¹¹ Takashi Kobayashi,⁹ Hiroshi Date,⁸ and Etsuro Hatano¹

¹Department of Surgery, Kyoto University Graduate School of Medicine, Sakyo-ku, Kyoto 606-8501, Japan

²Department of Neurology, Kyoto University Graduate School of Medicine, Sakyo-ku, Kyoto 606-8501, Japan

³Advanced Comprehensive Research Organization, Teikyo University, Itabashi-ku, Tokyo 173-8605, Japan

⁴Division of Sleep Medicine, Kansai Electric Power Medical Research Institute, Fukushima-ku, Osaka 553-0003, Japan

⁵Department of Hematology and Oncology, Kyoto University Graduate School of Medicine, Sakyo-ku, Kyoto 606-8501, Japan

⁶Department of Hematology and Oncology, Research Institute for Radiation Biology and Medicine, Hiroshima University, Hiroshima 734-8553, Japan

⁷Department of Hepato-Biliary-Pancreatic Surgery and Transplantation, Kanazawa University, Kanazawa 920-8640, Japan

⁸Department of Thoracic Surgery, Kyoto University Graduate School of Medicine, Sakyo-ku, Kyoto 606-8501, Japan

⁹Department of Urology, Kyoto University Graduate School of Medicine, Sakyo-ku, Kyoto 606-8501, Japan

¹⁰Center for Kidney Disease and Transplantation, Akita University Hospital, Akita 010-0041, Japan

¹¹Department of Urology, Akita University Graduate School of Medicine, Akita 010-8543, Japan

¹²Department of Clinical Laboratory, Kyoto University Hospital, Sakyo-ku, Kyoto 606-8507, Japan

¹³Education and Research Center for Community Medicine, Faculty of Medicine, Saga University, Saga 849-8501, Japan

¹⁴These authors contributed equally

¹⁵Lead contact

*Correspondence: takeros@kuhp.kyoto-u.ac.jp

<https://doi.org/10.1016/j.xcrm.2025.102153>

SUMMARY

Donor-specific antibodies (DSAs) against human leukocyte antigen (HLA) play a crucial role in antibody-mediated rejection, a major barrier to successful organ transplantation. Donor-recipient HLA molecular incompatibility critically influences DSA susceptibility, commonly assessed by analyzing mismatches in the HLA eplet repertoire. This study, including six distinct liver, lung, and kidney transplant cohorts from two centers (978 donor-recipient pairs), explores associations between individual eplet mismatches and DSA development. Certain mismatched eplets are strongly linked to DSA development, while others show weaker associations, a trend consistent across different organ types. Machine learning leverages these hierarchical associations to develop an eplet risk score (ERS), outperforming traditional eplet mismatch assessments. Furthermore, T cell proliferation in mixed lymphocyte reaction *in vitro* correlates with the ERS, attenuated by antibody-mediated inhibition of a mismatched DSA-associated eplet. These results establish the differential immunological impacts of mismatched HLA eplets as integral in clinical practice and therapeutic innovation.

INTRODUCTION

Solid organ transplantation represents the only curative treatment for patients suffering from end-stage organ failure. Advancements in the perioperative management of grafts and patients have led to a remarkable extension of survival. However, mitigating alloimmune reactions post-transplantation in the long-term remains a significant challenge. Even though considerable progress has been made in immunosuppressive agents that alleviate T cell-mediated rejection,^{1,2} standardized treatment strategies to counter anti-

body-mediated rejection (AMR) remain unestablished in organ transplantation.^{3–6} A distinguishing feature of AMR is the development of donor-specific antibody (DSA) against human leukocyte antigens (HLAs), particularly HLA class II molecules.^{7–11} DSA develops in 10%–50% of organ transplant recipients, resulting in graft injury and failure.^{7–13} While the presence of DSA does not necessarily lead to AMR, the ability to anticipate the emergence of DSAs and subsequently mitigate their occurrence holds significant promise in enhancing the overall prognosis associated with organ transplantation.



The primary role of HLA molecules is to present antigenic peptides on the cell surface. The HLA system has evolved to be highly polymorphic to accommodate a vast number of foreign antigens in humans.¹⁴ Nevertheless, in organ transplantation, HLA polymorphisms frequently cause antigenic incompatibility between donors and recipients.¹⁵ Consequently, mismatched donor HLA molecules are targeted by the recipient's immune system as non-self-antigens, triggering alloimmune reactions and DSA development. Traditional assessments of HLA compatibility have relied on comparing serological HLA antigens or genetically defined HLA alleles.¹⁵ Yet, these methods have not demonstrated sufficient predictive accuracy for DSA development for reliable clinical application.^{16,17} This limitation is attributed to their qualitative focus on merely discerning whether donor and recipient HLA types are identical or different. However, considering the substantial variability in the structural alignment of mismatched HLA molecules—ranging from nearly identical to significantly divergent—it becomes imperative to incorporate a quantitative evaluation of the structural differences of HLA molecules for a more precise assessment of HLA incompatibility between donors and recipients.

The long-standing recognition that antisera reactive to specific HLA antigens often cross-react with unrelated HLA antigens led to the development of the cross-reactive antigen groups concept.^{18–21} This concept further refines the understanding of “HLA epitopes,” defined as antibody recognition sites on HLA molecules.^{20–22} Many of these epitopes, more precisely termed B cell epitopes, are hypothesized to exist simultaneously on a single HLA molecule, and those sharing the same epitopes are presumed to elicit a similar response to antisera.^{23,24} These epitopes were initially defined conceptually, and, with time, the assessment of HLA eplets, defined as small clusters of polymorphic amino acids that determine antibody-binding specificity to HLA, has become a standard method for evaluating HLA epitopes on individual HLA molecules.²⁵ These eplets were first defined based on the three-dimensional structural topography of HLA molecules, with the eplet repertoire continuously updated by integrating data from *in vitro* antibody binding assays (<https://www.epregistry.com.br>).^{26,27} A growing body of evidence suggests that HLA incompatibility at the eplet level, as determined by the number of eplet mismatches, carries greater clinical significance than incompatibility at the antigen or allele levels for DSA development.^{16,17,28,29} Yet, several questions persist regarding the immunological significance of HLA eplets. Although recent reports have suggested that the risk of DSA development posed by individual HLA eplet mismatches varies among eplets,^{30–34} the precise degree of risk associated with each specific eplet remains uncertain, and it is still unclear whether this risk differs across transplants involving different organs or remains consistent. Moreover, the immunogenicity of individual HLA eplet mismatches, that is, the extent to which each mismatched HLA eplet incites an alloimmune response, has not been conclusively validated through experimental means.

In this study, we have assembled comprehensive clinical data from two transplant centers, encompassing 978 donor-recipient pairs spanning six distinct liver, lung, and kidney transplant cohorts. These data were synergized with *in vitro* experimental analyses to address the aforementioned questions. Our analysis

revealed a consistent pattern in the hierarchy of eplet mismatches across various solid organ transplants in terms of their impact on DSA development. Capitalizing on this discovery, we have leveraged this hierarchy to create an “eplet risk score (ERS),” which accurately predicted DSA development across different solid organs. Furthermore, through T cell activation assessments in a mixed lymphocyte reaction (MLR), we experimentally validated the immunological significance of this shared hierarchy and high potential of mismatched eplets clinically associated with DSA development. This integrated approach underscores the broad biological relevance of eplet mismatches across diverse solid organs and contributes to improve organ transplantation outcomes.

RESULTS

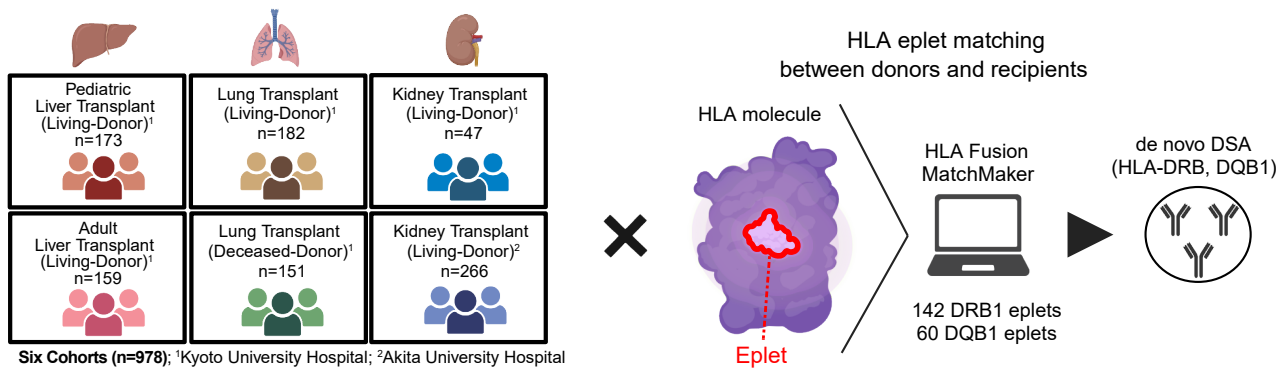
Baseline characteristics of six solid organ transplant cohorts

We enrolled a total of 893 cases, corresponding to 978 donor-recipient pairs, from six distinct cohorts. This included two cohorts, each from liver and lung transplantation, and one cohort from kidney transplantation at Kyoto University Hospital, in addition to another kidney transplant cohort from Akita University Hospital. The study flowchart is presented in [Figure S1](#). Among the cases, 99.8% were Japanese. The baseline characteristics of each cohort are described in [Table S1](#). The eplet composition of donors and recipients, as well as the mismatched eplets in each cohort, is described in [Table S2](#). A schematic representation of the three-step analytical approach utilized in this study is presented in [Figure 1](#).

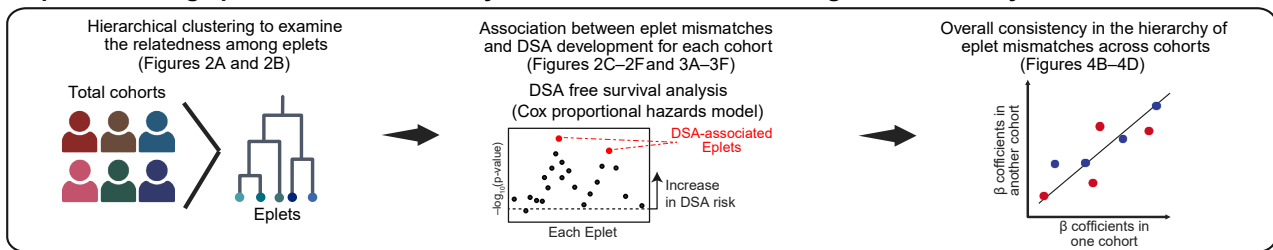
Association between individual eplet mismatches and DSA development

In this study, we focused on the DSA against HLA class II. Given the intricate relationships among eplets due to the linkage disequilibrium (LD), we first employed hierarchical clustering to examine the relatedness of 105 HLA-DRB1 (DR beta 1) and 55 HLA-DQB1 (DQ beta 1) eplets, which were identified as mismatched at least once in patients who developed DSA, using the Jaccard index (JI) ([Figures 2A and 2B](#)).

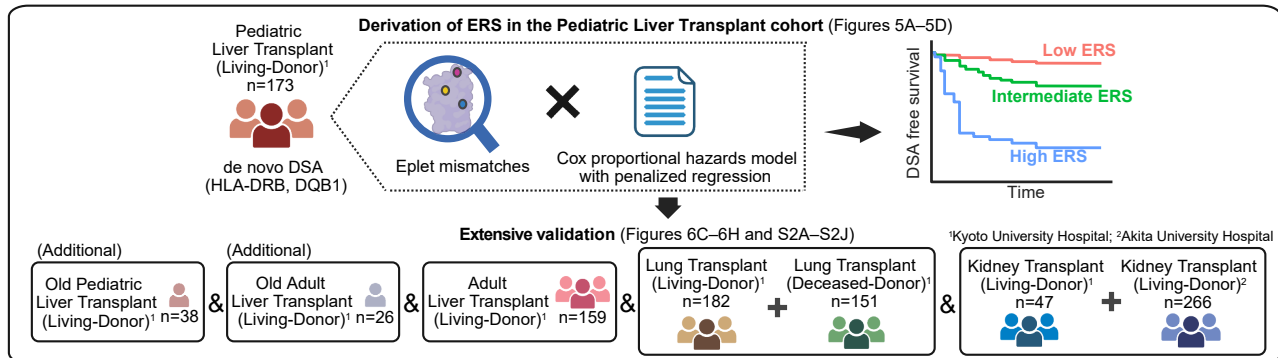
Next, for each cohort, we conducted a DSA-free survival analysis using the Cox proportional hazards model. This model examined the associations between individual eplet mismatches and the subsequent DSA development, adjusting for age and gender. In the pediatric living-donor liver transplant cohort (173 donor-recipient pairs), mismatches at 104AK, 98E, and 104A DRB1 eplets, which were invariably related as mismatched eplets in our cohorts (JI = 1.0), were found to be significantly associated with HLA-DR-DSA development, after adjusting for multiple testing (hazard ratio [HR] adjusted for age and gender [aHR-ag] = 5.6 [95% confidence interval (CI), 3.0–10.6], $p = 1.2 \times 10^{-7}$) ([Figure 2C](#)). For the DQB1 eplets, mismatches at the 52PL3 and 84QL3 eplets, which were highly related as mismatched eplets in our cohorts (JI = 0.95) and perfectly related in the pediatric living-donor liver transplant cohort, were most significantly associated with DQ-DSA development (aHR-ag = 5.2 [95% CI, 2.8–9.6], $p = 2.0 \times 10^{-7}$). Other DQB1 mismatched eplets that were also significantly associated with HLA-DQ-DSA



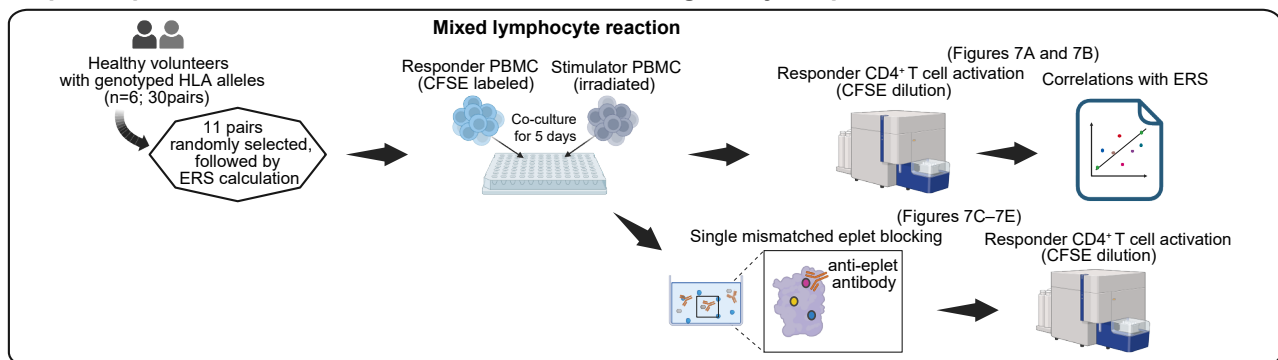
Step 1: Detecting eplet mismatch hierarchy within cohorts and assessing its consistency across cohorts



Step 2: Derivation and validation of the Eplet Risk Score (ERS)



Step 3: Experimental validation of ERS and the immunogenicity of eplet mismatches



(legend on next page)

development included 55PP, 185I, 45EV, 55RL3, 185T, 116V, 52PQ2, 140A2, 66ER, 52PR, 74SV2, 75V, 23L, and 55PPD (Figure 2D; Table S3).

In the adult living-donor liver transplant cohort (159 donor-recipient pairs), none of the DRB1 eplet mismatches reached statistical significance in relation to DR-DSA development (Figure 2E). The DQB1 mismatched eplets that were significantly associated with DQ-DSA development included 52PL3 (aHR-ag = 4.6 [95% CI, 2.0–10.6], $p = 2.7 \times 10^{-4}$), 55RL3, and 84QL3 (Figure 2F; Table S3).

In the living-donor lung transplant cohort (182 donor-recipient pairs), while none of the DRB1 mismatched eplets reached statistical significance (Figure 3A), mismatches at five DQB1 eplets were significantly associated with DQ-DSA development: 23R (aHR-ag = 153.1 [95% CI, 23.0–1,017.0], $p = 1.9 \times 10^{-7}$), 56P, 67VT, 66EV, and 185T (Figure 3B; Table S3).

In the deceased-donor lung transplant cohort (151 donor-recipient pairs), mismatches at four DRB1 eplets, namely, 85A, 38L, 28EH, and 37L, which were invariably related as mismatched eplets in our cohorts (JI = 1.0), were significantly associated with DR-DSA development (aHR-ag = 19.5 [95% CI, 4.3–89.8], $p = 1.3 \times 10^{-4}$) (Figure 3C; Table S3). The DQB1 mismatched eplets that were significantly associated with DQ-DSA development included 45EV (aHR-ag = 5.6 [95% CI, 2.4–13.2], $p = 6.1 \times 10^{-5}$), 55PP, 55PPD, 9Y, and 84QL3 (Figure 3D; Table S3).

In the kidney transplant cohort from Akita University Hospital (266 donor-recipient pairs), none of the DRB1 and DQB1 mismatched eplets achieved statistical significance (Figures 3E and 3F). We opted not to perform this analysis on the kidney transplant cohort from Kyoto University Hospital due to the extremely low incidence of DSA development (event number = 2 [DR-DSA] and 2 [DQ-DSA]).

These findings showed that certain eplets demonstrate a markedly potent correlation with DSA development, while others show a comparatively weaker association, thereby underscoring a hierarchical structure in the influence of eplet mismatches on DSA emergence. Eplet mismatches that were initially associated with DSA development but did not retain statistical significance after Bonferroni correction are listed in Table S4.

Overall consistency in the hierarchy of eplet mismatches across five cohorts of liver, lung, and kidney transplantations

While mismatched eplets significantly associated with DSA development were not always consistent across cohorts (Figure 4A), this analysis discarded information of most mismatched eplets. Therefore, we conducted a weighted correlation analysis of the β coefficients obtained through the Cox proportional hazards model. Notably, significant positive correlations surfaced among diverse cohorts, regardless of whether they involved the same organ (Figure 4B) (e.g., liver-pediatric vs.

liver-adult, Pearson correlation coefficients [r_p] = 0.31, $p = 4.3 \times 10^{-4}$; lung, living-donor vs. lung, deceased-donor $r_p = 0.59$, $p = 8.2 \times 10^{-9}$) or different organs (e.g., liver-pediatric vs. lung, living-donor, $r_p = 0.39$, $p = 2.2 \times 10^{-4}$ [Figure 4C]; liver-adult vs. lung, deceased-donor, $r_p = 0.37$, $p = 5.3 \times 10^{-5}$; lung, deceased-donor vs. kidney, living-donor [Akita University Hospital], $r_p = 0.50$, $p = 1.8 \times 10^{-7}$ [Figure 4D]).

These observations suggested that the hierarchical association between eplet mismatches and DSA development was conserved across the five cohorts, highlighting the universal importance of the hierarchy among eplet mismatches across different types of organ transplantations. Nevertheless, the observed non-concordance among mismatched eplets significantly associated with DSA development also raised the possibility of organ-specific variations.

Quantification of the degree of eplet mismatching and its relationship with DSA development

To measure the overall risk of DSA development in each transplant pair while accounting for the hierarchy among eplet mismatches, a machine learning approach was employed, combining the Cox proportional hazards model with penalized regression models.^{35,36} The eplet mismatches in HLA-DRB1 and HLA-DQB1 were used to construct the model for DR-DSA and DQ-DSA development, respectively. The pediatric living-donor liver transplant cohort (173 donor-recipient pairs, follow-up = 6.5 years [interquartile range (IQR), 3.4–9.2]; event number = 49 [DR-DSA] and 55 [DQ-DSA]) was chosen as the derivation cohort because it had the largest event number (i.e., DSA development) of all our cohorts. Of the three penalized regression models, we selected the ridge model because it demonstrated better accuracy in the derivation cohort than the lasso and elastic net models (Table S5). We then calculated the score for each transplant pair, termed as the “ERS for DR-DSA” (DR-ERS) and the “ERS for DQ-DSA” (DQ-ERS), by applying the weighted sum of individual eplet mismatches, with weights determined using the ridge model (Figures 5A and 5B; specific weights are presented in Table S6). Additionally, we have made a web-based application available for easy ERS calculation at https://erscalculator.shinyapps.io/ers_application_deploy/.

In the derivation cohort, even after adjusting for the number of eplet mismatches, DR-ERS accurately predicted DR-DSA development (HR adjusted for age, gender, and the number of eplet mismatches for one point increase [aHR-agen] = 7.9 [95% CI, 4.7–13.4], $p = 1.7 \times 10^{-14}$) (Figure 5C), and DQ-ERS accurately predicted DQ-DSA development (aHR-agen = 6.3 [95% CI, 3.7–10.6], $p = 6.2 \times 10^{-12}$) (Figure 5D). *Post hoc* analyses suggested that, based on the 1-year cumulative event incidence rates calculated via Kaplan-Meier analysis—0.10 for DR-DSA and 0.13 for DQ-DSA—the estimated cumulative outcome incidence CIs were calculated to be 0.114 for DR-DSA and 0.118 for

Figure 1. Study overview

The study is structured around three primary steps. Step 1 aims to identify the hierarchy of eplet mismatches within cohorts and to evaluate its reproducibility across different cohorts. Step 2 is dedicated to the development and validation of the eplet risk score (ERS). Step 3 involves experimentally validating the ERS and examining the immunogenicity of eplet mismatches identified through clinical analysis as potential drivers of donor-specific antibody risk. HLA, human leukocyte antigen; PBMC, peripheral blood mononuclear cell; CFSE, carboxyfluorescein diacetate succinimidyl ester. The figure was created with BioRender.com.

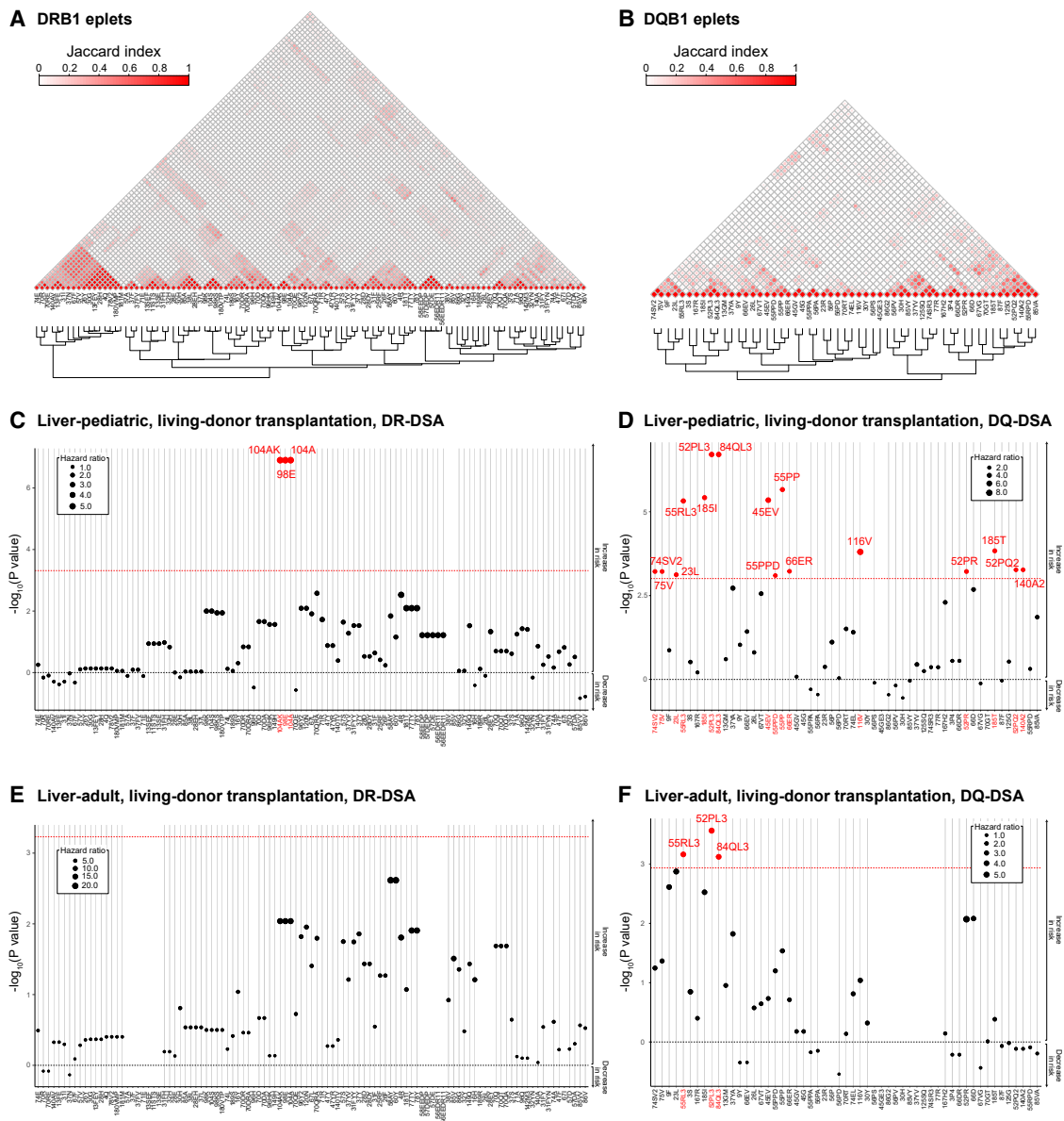


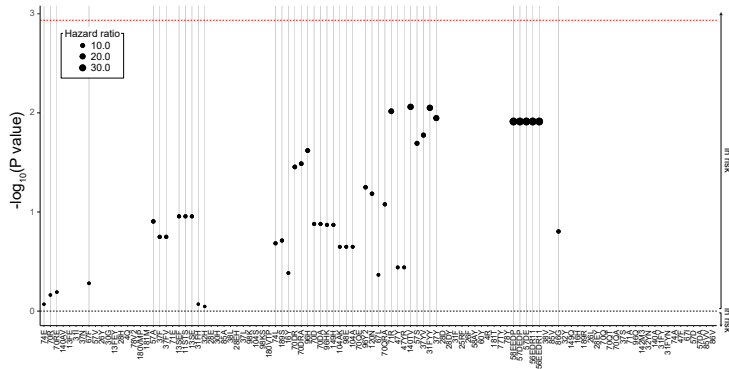
Figure 2. Intricate relationships among eplet mismatches and their association with donor-specific antibody development in liver transplants

We clustered 105 HLA-DRB1 and 55 HLA-DQB1 eplet mismatches using the hierarchical clustering based on the Jaccard index (JI) between each pair of mismatched eplets. Complex relatedness between mismatched eplets was visualized using dendrograms with triangular matrixes (A and B). A higher JI value, approaching 1, indicates a higher likelihood of concurrent detection of the paired mismatched eplets. Survival analysis results, assessed via the Cox proportional hazards model accounting for age and gender, are represented in Manhattan-style plots (C–F). Eplets without associated dots were never identified as mismatched in patients who developed DSA in the respective cohorts. The graph has been inverted around the $y = 0$ horizontal line, so eplet mismatches linked to a lower risk of DSA development (i.e., hazard ratio [HR] < 1) are depicted below the $y = 0$ horizontal line. The red dotted line indicates the threshold for statistical significance in each cohort, and eplets reaching statistical significance are highlighted in red. Eplets with a high JI generally exhibited similar p values (y axis) and age-gender adjusted HR (indicated by dot size). Donor-recipient pairs, $n = 173$ (pediatric living-donor liver transplant cohort) and 159 (adult living-donor liver transplant cohort). p values were derived using the Wald test, calculated by dividing the β coefficient by its standard error.

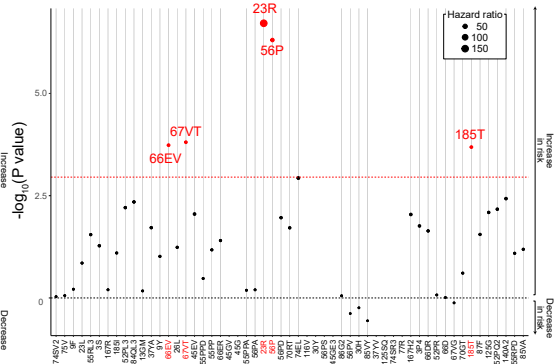
DQ-DNA, which we consider to be within an acceptable range.³⁷ To validate the ERS in independent pediatric living-donor liver transplant cases, we evaluated it in 38 pediatric cases who underwent liver transplantation at Kyoto University Hospital prior to the recruitment period of the original cohort (Figure S1;

Table S1). Since this cohort predated the implementation of routine anti-HLA antibody testing, many patients did not undergo pre-transplant anti-HLA antibody testing. Nevertheless, the ERS demonstrated robust predictive power with both DR-ERS and DQ-ERS effectively forecasting DR-DNA and DQ-DNA,

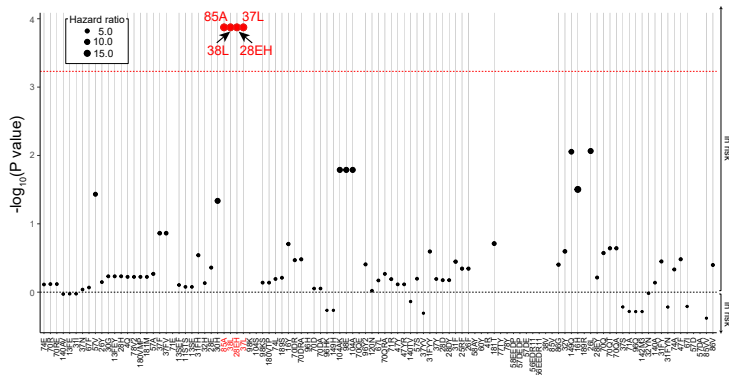
A Lung, living-donor transplantation, DR-DSA



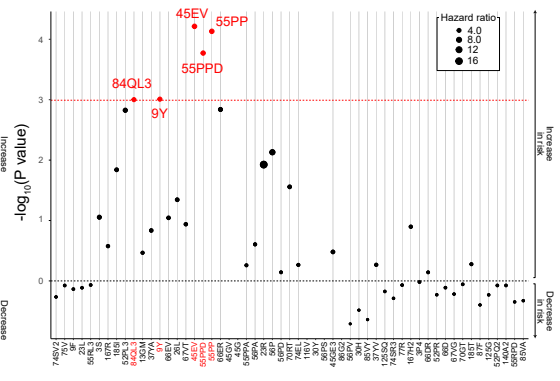
B Lung, living-donor transplantation, DQ-DSA



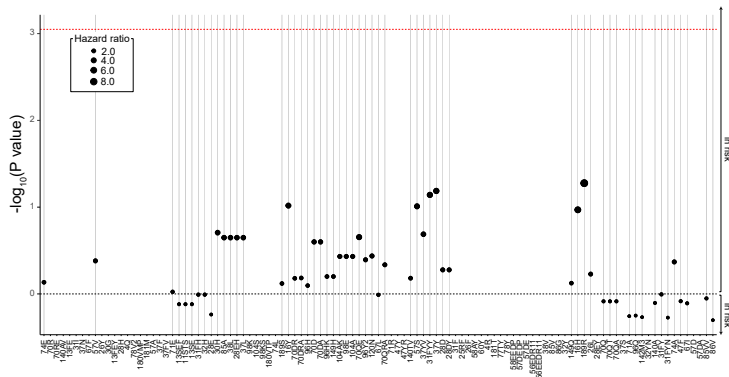
C Lung, deceased-donor transplantation, DR-DSA



D Lung, deceased-donor transplantation, DQ-DSA



E Kidney (Akita), living-donor transplantation, DR-DSA



F Kidney (Akita), living-donor transplantation, DQ-DSA

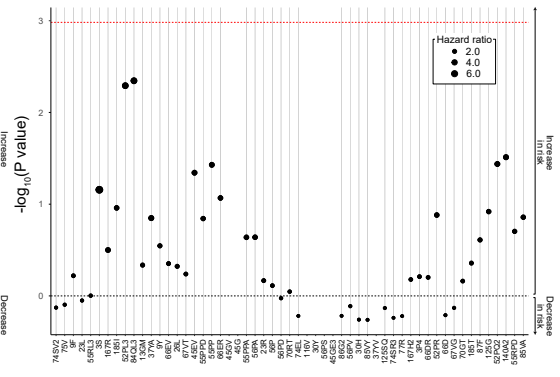


Figure 3. Association between individual eplet mismatches and donor-specific antibody development in lung and kidney transplants

The results of survival analysis, evaluated using the Cox proportional hazards model adjusting for age and gender, are displayed in Manhattan-style plots (A–F), as described in the legend for Figure 2. Eplets that exhibited a high Jaccard index (JI) typically presented similar p values (as shown on the y axis) and hazard ratios (HRs) adjusted for age and gender (as indicated by the size of the dots). p values were calculated using the Wald test, dividing the β coefficient by its standard error. Donor-recipient pairs, $n = 182$ (living-donor lung transplant cohort), 151 (deceased-donor lung transplant cohort), and 266 (kidney transplant cohort from Akita University Hospital). p values were derived using the Wald test, calculated by dividing the β coefficient by its standard error.

respectively (DR-DSA, aHR-agen = 5.8 [95% CI, 1.7–19.3], $p = 4.3 \times 10^{-3}$; DQ-DSA, aHR-agen = 2.5 [95% CI, 1.3–5.0], $p = 7.0 \times 10^{-3}$) (Figures S2A and S2B).

We proceeded to validate the DR-ERS and DQ-ERS with other cohorts from liver, lung, and kidney transplant cases enrolled from two transplant centers. The deceased-donor lung trans-

plant cohort exhibited a higher ERS distribution (Figures 6A and 6B), likely due to receiving organs from non-blood relatives. In the adult living-donor liver transplant cohort (159 donor-recipient pairs, follow-up = 6.2 years [IQR, 3.4–9.1], event number = 6 [DR-DSA] and 24 [DQ-DSA]), both DR-ERS and DQ-ERS accurately predicted the development of DR-DSA and DQ-DSA,

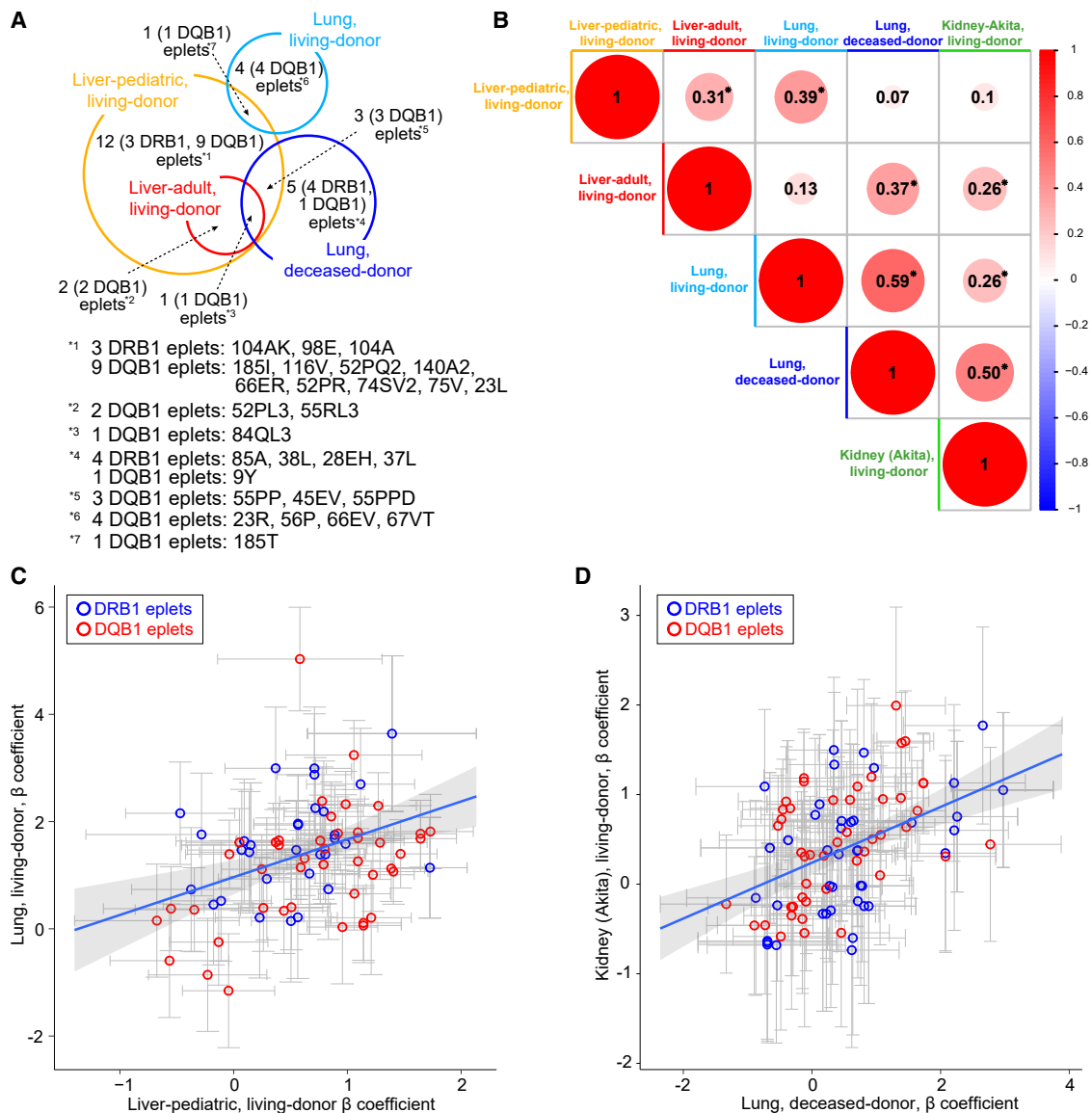


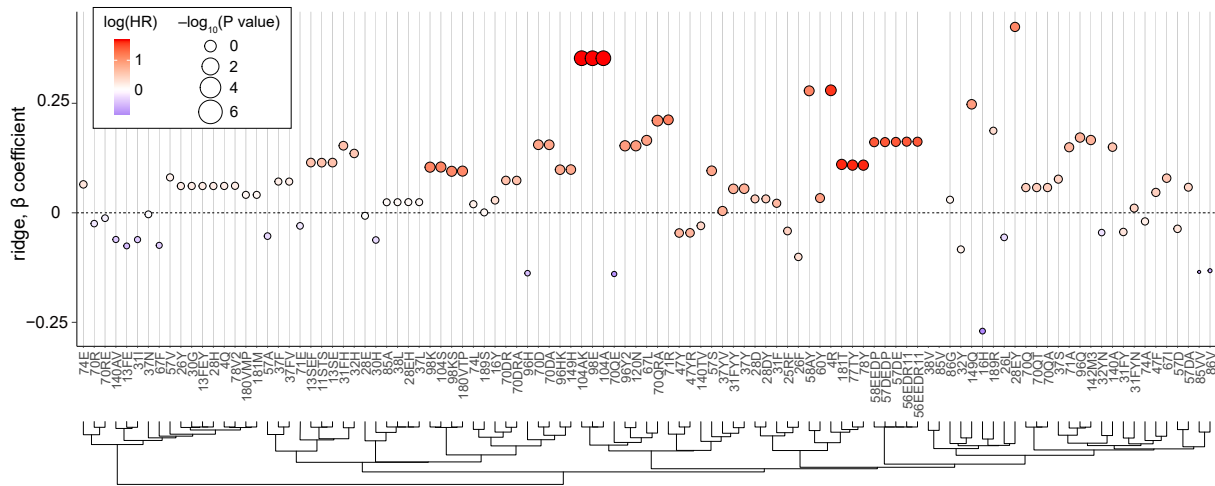
Figure 4. Overall consistency in the hierarchy of eplet mismatches across five cohorts of liver, lung, and kidney transplants

Eplet mismatches significantly associated with donor-specific antibody (DSA) development were not always concordant across the different cohorts (A). However, when considering β coefficients of all eplet mismatches, the general pattern of associations between each eplet mismatch and DSA development demonstrated notable correlations across various cohorts (B). Representative scatterplots (C and D) present the associations between the β coefficients derived from two cohorts indicated at the labels of x axis and y axis. A p value less than 5.0×10^{-3} (Bonferroni-corrected statistical significance threshold) is indicated by an asterisk (*). In the weighted correlation analysis, p values were obtained using the t test for the correlation coefficient (r_p). Error bars denote standard errors, while the gray area represents the 95% confidence intervals (CIs) of the regression lines.

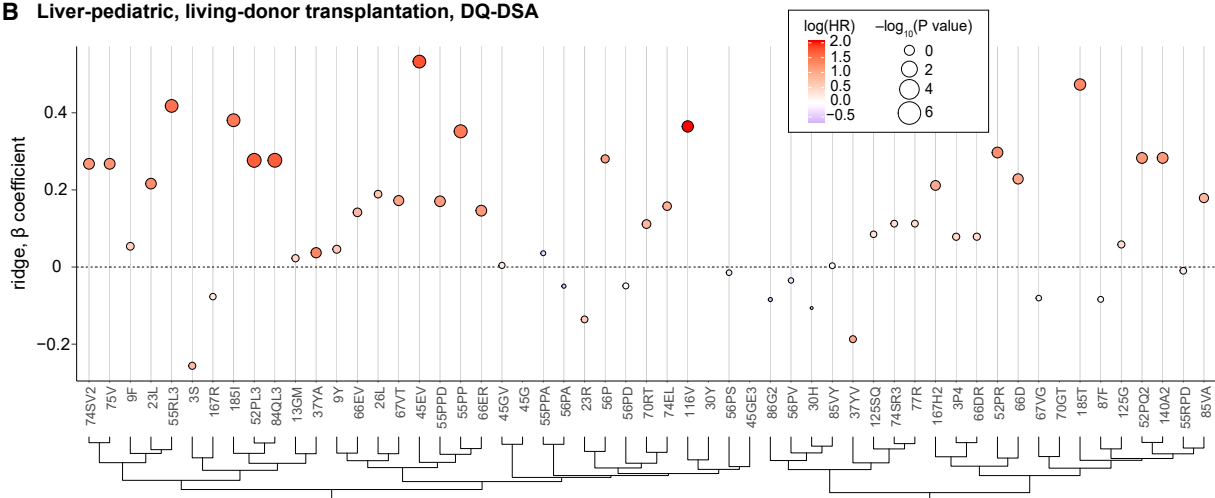
respectively (DR-ERS, aHR-agen = 83.2 [95% CI, 4.0–1745.6], $p = 4.4 \times 10^{-3}$; DQ-ERS, aHR-agen = 7.5 [95% CI, 3.1–18.3], $p = 9.9 \times 10^{-6}$) (Figures 6C and 6D). The applicability of the ERS to adult living-donor liver transplant cases was further confirmed by evaluating it in 26 adult cases who underwent liver transplantation at Kyoto University Hospital prior to the recruitment period of the original cohort (DR-DSA, aHR-agen = 10.0 [95% CI, 1.8–55.6], $p = 8.3 \times 10^{-3}$; DQ-DSA, aHR-agen = 6.7 [95% CI, 1.3–35.0], $p = 2.5 \times 10^{-2}$) (Figures S1, S2C, and S2D; Table S1).

A similar pattern emerged in the living-donor lung transplant cohort (182 donor-recipient pairs, follow-up = 4.5 years [IQR, 1.8–7.2], event number = 5 [DR-DSA] and 11 [DQ-DSA]), with both DR-ERS and DQ-ERS showing significant predictive capability for DR-DSA and DQ-DSA development, respectively (DR-DSA, aHR-agen = 8.7 [95% CI, 1.2–61.9], $p = 0.03$; DQ-DSA, aHR-agen = 5.0 [95% CI, 1.7–15.0], $p = 3.8 \times 10^{-3}$) (Figures S2E and S2F). In the deceased-donor lung transplant cohort (151 donor-recipient pairs, follow-up = 3.1 years [IQR, 1.6–5.0], event number = 8 [DR-DSA] and 22 [DQ-DSA]), the

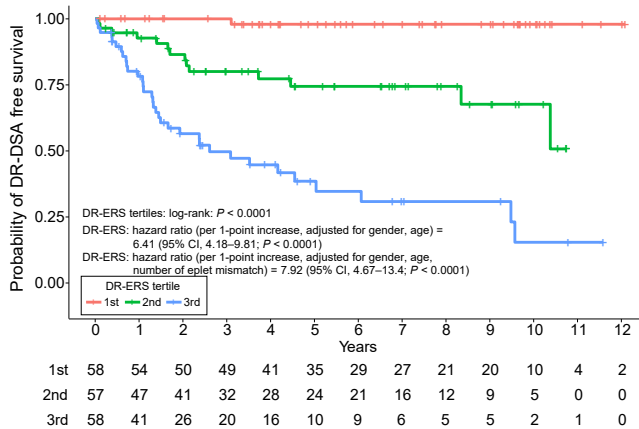
A Liver-pediatric, living-donor transplantation, DR-DSEA



B Liver-pediatric, living-donor transplantation, DQ-DSEA



C Liver-pediatric, living-donor transplantation, DR-DSEA



D Liver-pediatric, living-donor transplantation, DQ-DSEA

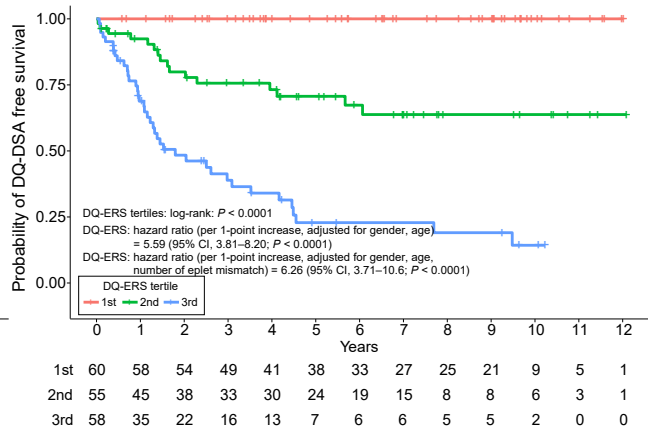


Figure 5. Eplet risk score derivation using pediatric living-donor liver transplant cohort

We employed the ridge model to assess the relationship between individual eplet mismatches and donor-specific antibody (DSA) development. Manhattan-style plots illustrate β coefficients, which served as the weights in the final model to compute the ERS for DR-DSEA (DR-ERS) (A) and DQ-DSEA (DQ-ERS) (B). These are

(legend continued on next page)

DR-ERS did not achieve statistical significance in predicting DR-DSA development (aHR-agen = 3.4 [95% CI, 0.8–15.0], $p = 0.11$) (Figure S2G), likely due to large CIs resulting from scarce event occurrence. Yet, the DQ-ERS significantly predicted DQ-DSA development (aHR-agen = 2.9 [95% CI, 1.4–6.1], $p = 3.5 \times 10^{-3}$) (Figure S2H). When the two lung cohorts were combined, the predictive accuracy remained consistent (DR-DSA, aHR-agen = 3.3 [95% CI, 1.1–9.4], $p = 0.03$; DQ-DSA, aHR-agen = 3.4 [95% CI, 1.9–5.9], $p = 3.3 \times 10^{-5}$) (Figures 6E and 6F).

In the living-donor kidney transplant cohort from Akita University Hospital (266 donor-recipient pairs, follow-up = 7.5 years [IQR, 3.9–11.9], event number = 7 [DR-DSA] and 14 [DQ-DSA]), the predictive power of the DR-ERS did not reach statistical significance (aHR-agen = 2.8 [95% CI, 0.7–12.0], $p = 0.15$) (Figure S2I), likely due to an insufficient number of events. Meanwhile, the DQ-ERS significantly predicted DQ-DSA development (aHR-agen = 2.7 [95% CI, 1.0–6.9], $p = 0.04$) (Figure S2J). When the living-donor kidney transplant cohort from Kyoto University Hospital (47 donor-recipient pairs, follow-up = 5.8 years [IQR, 4.3–8.7], event number = 2 [DR-DSA] and 2 [DQ-DSA]) was combined, the predictive ability of DR-ERS reached statistical significance (aHR-agen = 3.5 [95% CI, 1.0–11.9], $p = 0.048$) (Figure 6G). DQ-ERS was consistent in significantly predicting DQ-DSA (aHR-agen = 3.4 [95% CI, 1.3–8.8], $p = 0.01$) (Figure 6H).

Importantly, the ERS consistently displayed stronger associations with DSA development compared to the traditional method of assessing epitope mismatch via the number of eplet mismatches in all cohorts studied. Upon adjusting for the ERS, the number of eplet mismatches was not significantly associated with an increased risk of DSA development in any of the cohorts (Table S7). Additionally, including variables such as the number of acute rejection episodes during the follow-up period, the number of acute rejections within the first year post-transplant, the number of immunosuppressive drugs (at the time of DSA onset for those who developed DSA and at the last follow-up for those who did not), the number of immunosuppressive drugs at the 1-year mark post-transplant, the inclusion of calcineurin inhibitors among these drugs, and the number of HLA antigen mismatches—along with age, gender, and the number of eplet mismatches—did not significantly impact the predictive ability of the ERS for DSA development (Table S8).

Collectively, our findings demonstrated that both DR-ERS and DQ-ERS offered a more precise quantification of DSA development risk per transplant pair compared to a conventional method of counting eplet mismatches. This affirmed the presence of a hierarchy in eplet mismatch's predictive power for DSA development, a principle applicable across various organ transplants.

Additionally, after finding that statistically significant eplets were significantly more likely to be “antibody-verified” eplets

(Figures S3A and S3B), we analyzed whether confining the model to “antibody-verified” eplets would enhance the predictive performance of our ERS. Contrary to expectations, however, this confinement reduced the predictive ability of our ERS models (Figures S3C and S3D).

ERS is associated with alloreactive T cell proliferation in MLR

To verify the significance of ERS in alloimmune reaction, we next examined whether ERS correlates with activation of responder T cells in *in vitro* MLR. We isolated peripheral blood mononuclear cells (PBMCs) from two of a pool of HLA-mismatched healthy volunteers (Table S9) and used them as stimulator and responder cells in MLR (see STAR Methods); 11 pairs of stimulators and responders were selected at random (Table S9). Notably, even after adjusting for the number of eplet mismatches, the total ERS—calculated by combining DR-ERS and DQ-ERS—remained strongly correlated with CD4⁺ T cell activation status, as indicated by the percentage of carboxyfluorescein diacetate succinimidyl ester (CFSE)^{low} CD4⁺ T cells (partial Spearman's rank correlation coefficient [ρ_p] = 0.75, $p = 0.014$) (Figures 7A and 7B). Correlations between total ERS and the percentages of CFSE^{low} CD8⁺ T cells were less evident ($\rho_p = 0.29$, $p = 0.42$). By contrast, there were no significant associations between the number of eplet mismatches and all examined MLR parameters (Table S10).

Blocking a DSA-associated eplet suppresses alloreactive T cell proliferation

Finally, antibody blocking experiments were performed to determine whether eplet mismatches associated with DSA development are indeed potent triggers for alloimmune reactions. The 55PP in HLA-DQB1 was targeted because this mismatch was strongly associated with DSA development in our cohorts (i.e., pediatric living-donor liver transplant and the deceased-donor lung transplant cohorts; Figures 2D and 3D). PBMCs from one pair of HLA-mismatched healthy volunteers (pair #4; Table S9), which had a 55PP mismatch on HLA-DQB1, were selected as stimulators and responders in the MLR. A monoclonal antibody against 45EV was also selected as control as this eplet was not mismatched in this stimulator-responder pair. Notably, the anti-55PP antibody significantly decreased the percentage of CFSE^{low} CD4⁺ T cells in a dose-dependent manner (Figure 7C), when used at concentrations above 1×10^2 ng/mL (Figure 7D). In contrast, the anti-45EV antibody did not affect CD4⁺ T cell proliferation (Figure 7E).

Collectively, these results provide compelling experimental evidence of the hierarchy among eplet mismatches in triggering alloimmune reaction and demonstrate that a DSA-associated eplet mismatch itself can cause alloreactive T cell proliferation.

represented on the y axis. The dot size corresponds to the log₁₀-transformed p value, and color indicates the log-transformed hazard ratio (HR) from the primary analysis. Kaplan-Meier analysis verified that both DR-ERS and DQ-ERS accurately predicted DR-DSA and DQ-DSA development, respectively, in the pediatric living-donor liver transplant cohort (C and D). For ease of visualization, patients were stratified into three groups based on ERS tertiles: the DR-ERS tertile values were 0.22 and 0.87, and the DQ-ERS tertile values were 0.00 and 1.22. Donor-recipient pairs, $n = 173$ (pediatric living-donor liver transplant cohort). p values in the Kaplan-Meier analysis were derived from the log rank (Mantel-Cox) test, while those for HR came from the Wald test of the Cox proportional hazard model. In the Kaplan-Meier plots, vertical lines represent censored cases.

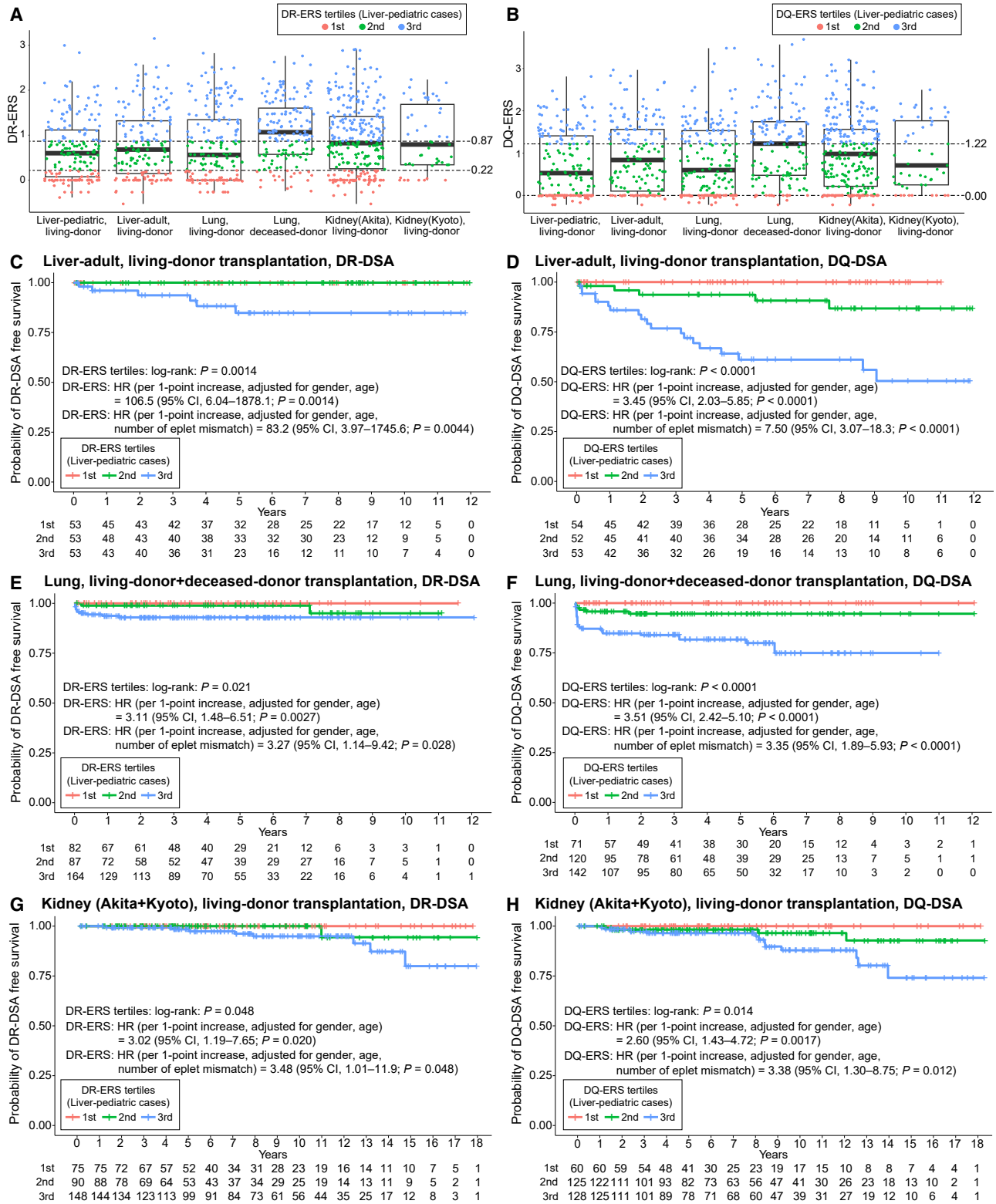


Figure 6. Eplet risk score validation in independent cohorts from liver, lung, and kidney transplantations across two transplant centers
Boxplots show the distribution of the DR-ERS (A) and the DQ-ERS (B) values in six distinct cohorts compiled in this study. Participants were stratified into three groups according to their DR-ERS and DQ-ERS tertile values derived from the pediatric living-donor liver transplant cohort for Kaplan-Meier analyses. These

(legend continued on next page)

DISCUSSION

In this study, we executed a comprehensive analysis that ranged from large clinical datasets acquired from two Japanese transplant centers to *in vitro* validation. This allowed us to identify a cross-organ hierarchy of HLA eplets, which determined the susceptibility of DSA development following organ transplantation, regardless of the organ type. Crucially, our application of machine learning to leverage this HLA eplet hierarchy resulted in a significant improvement in the accuracy of DSA development prediction. Moreover, our *in vitro* findings corroborated the existence of this eplet hierarchy and affirmed the immunological significance of eplets highly associated with DSA development as potent inducers of alloimmune reactions. Importantly, we provide a web-based application to easily calculate ERS, available at https://erscalculator.shinyapps.io/ers_application_deploy/.

We believe that the clinical relevance of our findings is substantially high, given the established clinical importance of DSA development in solid organ transplantation. Prior studies have hinted at differential immunogenicity of eplet mismatches,^{30–34} yet the concept of quantifying these variations has been largely unexplored. Our results call for a paradigm shift toward acknowledging the need to quantify these immunological variations and leveraging them to accurately estimate each recipient's susceptibility to DSA development. We want to emphasize that one of the major strengths of our study lies in the unique characteristics of each cohort, with each cohort consisting of a homogeneous Japanese population and undergoing consistent immunosuppressive protocols and surgical procedures, attributable to being derived from the same institution and department (see [STAR Methods](#)). From the planning phase of our study, we recognized that variations in immunosuppressive protocols and surgical procedures could significantly impact DSA development,⁸ though these differences are challenging to quantify accurately as variables. Therefore, when estimating the risk of individual eplets, we focused our analyses within same-organ/same-center cohorts ([Figures 2 and 3](#)). Similarly, for the derivation of the ERS, we limited our analysis to a single-organ, single-center cohort (the pediatric liver transplant cohort at Kyoto University Hospital) ([Figure 5](#)). Additionally, we also validated the ERS exclusively within same-organ cohorts and, in most cases, within the same-center cohorts ([Figure 6](#)); we believe that this design has been pivotal in achieving the unprecedented resolution in estimating the differential immunogenicity of each eplet mismatch and DSA development. Importantly, this level of resolution has allowed us to reveal a consistent hierarchy of differential immunogenicity across various solid organs ([Figure 4B](#)). This finding of universality likely stems from the fact that HLA molecules are universally expressed by all organs.³⁸ However, we acknowledged that certain components of the eplet hierarchy still varied between organs ([Figure 4A](#)). Collectively, these results indicate that the hierarchy of eplets driving DSA risk comprises

both organ-shared and organ-specific components. Admittedly, while it was possible to observe overall trends in effect sizes, some cohorts lacked sufficient sample sizes and/or event numbers to identify “statistically significant” mismatched eplets ([Figures 2 and 3](#)). Therefore, larger sample sizes are warranted for further exploration to determine the extent to which organ-shared and organ-specific components contribute to DSA risk in different organs.

Interestingly, we observed notable differences in both the incidence and pattern of DSA development across the organ cohorts ([Figures 5 and 6](#)). In terms of incidence, the pediatric liver transplant cohort showed a higher DSA incidence than the other cohorts, which is consistent with previous reports.^{39,40} We assume that this increased incidence could be attributed to the lower levels of immunosuppression maintained in our pediatric liver transplant cohort, as immunosuppression in pediatric recipients at our institution is minimized to mitigate long-term side effects, particularly those affecting growth, development, and fertility.⁴¹ Regarding DSA development patterns, both the adult and pediatric living-donor liver transplant cohorts exhibited a gradual onset over time. In contrast, in the deceased-donor and living-donor lung transplant cohorts, DSA development was concentrated in the early post-transplant period, especially in deceased-donor transplants. We believe that inflammation in the graft, due to ischemia-reperfusion injury and prolonged ischemic times, may contribute to this earlier onset of DSA in the lung transplant cohorts.^{42,43} In contrast, in our living-donor kidney transplant cohort, DSA development was observed only in the late post-transplant period. This delayed onset of DSA in the kidney transplant cohort might be likely due to the typically stronger immunosuppressive regimens, including induction therapy, administered to kidney transplant recipients (see [STAR Methods](#)). Importantly, similar patterns have been reported in previous studies across liver, kidney, and lung transplants,^{9,28,44,45} suggesting that our findings align with established trends. While we have discussed several possible reasons, we acknowledge that there are likely yet undefined universal factors contributing to the observed differences in the incidence and pattern of DSA development across organ cohorts. Further research is needed to clarify these factors.

Mismatched donor HLA molecules are processed into donor-derived peptides by the antigen-presenting cells of the recipient. These peptides are subsequently presented to CD4⁺ T cells by HLA class II molecules. It has been widely assumed that this so-called “indirect” allorecognition by CD4⁺ T cells, which induces the subsequent activation and differentiation of B cells, is the main pathway implicated in DSA development.^{46–49} It should be noted that this dogma of the T cell allorecognition is based on limited experimental evidence and has been recently reconsidered because of the complexity of the alloimmune reaction.^{48,50,51} Moreover, several studies have reported that pathways other than the indirect pathway, such as the direct

analyses confirmed the association between ERS and DSA development in the adult living-donor liver transplant cohort (C and D), lung transplantation cohort (E and F), and kidney transplantation cohort (G and H). Donor-recipient pairs, $n = 159$ (adult living-donor liver transplant cohort), 333 (lung transplant cohort), and 313 (kidney transplant cohort). p values in the Kaplan-Meier analysis were calculated using the log rank (Mantel-Cox) test, while those for the hazard ratio (HR) were derived via the Wald test in the Cox proportional hazards model. In the boxplots, thick solid lines represent medians, boxes represent interquartile ranges (IQRs), and the error bars extending from the boxes represent the data within $1.5 \times$ IQR. Vertical lines in the Kaplan-Meier plots denote censored cases.

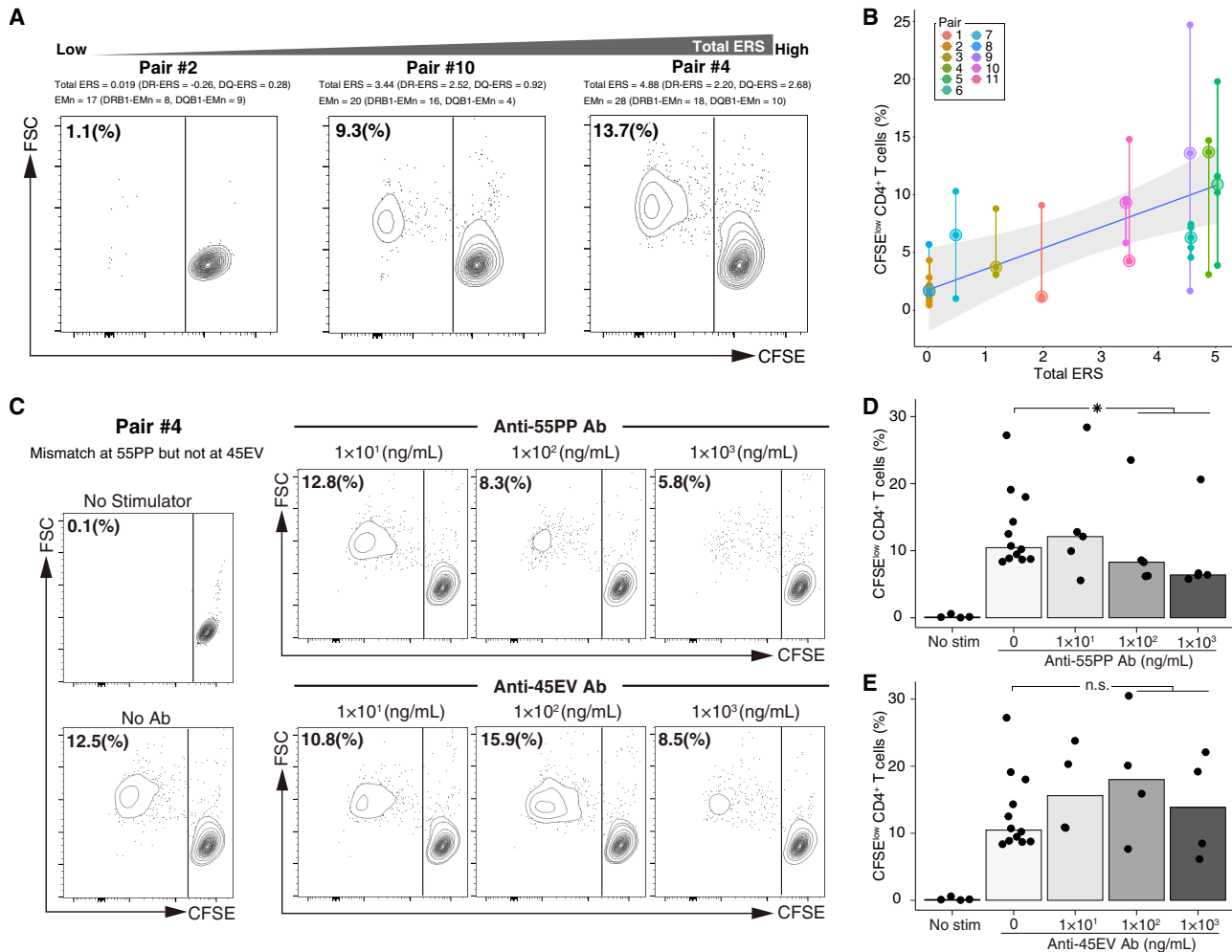


Figure 7. Examination of eplet mismatch immunogenicity in mixed lymphocyte reactions

The association between the eplet risk score (ERS) and the activation status of responder CD4⁺ T cells was analyzed. Representative scattergrams are shown in (A), and aggregated scatterplots are shown in (B). Each stimulator-responder pair was analyzed with 3–6 biological replicates. The effect of an anti-55PP antibody (Ab) or an anti-45EV Ab on the percentage of CFSE^{low} CD4⁺ T cells in the MLR was assessed using a stimulator-responder pair (pair #4, see Table S9). Representative scattergrams are shown in (C), and aggregated data are shown in (D) and (E). Each antibody concentration group was analyzed with 4–12 biological replicates. **p* < 0.05. *p* values were determined using the Wilcoxon rank-sum test, which compared the value at 0 ng/mL Ab with those at 1 × 10² and 1 × 10³ ng/mL Ab. EMn, the number of eplet mismatches; FSC, forward scatter; stim, stimulator. In the scatterplot shown in (B), large dots represent the median value of each stimulator-responder pair, small dots represent values obtained from each individual experiment, vertical lines represent ranges, and the gray area represents 95% confidence interval (CI) of the regression line. In the bar charts shown in (D) and (E), the top of the bar represents the median value, whereas the points represent values from individual experiments.

pathway, also play a critical role in DSA development.^{52–54} We acknowledge that the MLR assay used in this study is more apt for assessing the direct rather than the indirect pathway; however, precise assays for alloimmune reactions remain undeveloped. We showed that the ERS, but not the number of eplet mismatches, correlated with the activation status of CD4⁺ T cells in the MLR. Furthermore, we demonstrated that a monoclonal antibody targeting an eplet that was significantly associated with DSA development attenuated CD4⁺ T cell activation in a dose-dependent manner. We, therefore, maintain that our use of the MLR was appropriate for elucidating the immunological significance of eplet mismatches in this study. In this context, our *in vitro* work confirmed that ERS could quantify

the degree of alloimmune reactions potentially elicited in each transplant pair and that an eplet mismatch itself triggered these alloimmune reactions. However, future studies dedicated to understanding the underlying mechanisms of AMR, and creating a faithful *in vitro* model of it, remain a vital need.

We consider experimental verification to be critical, especially for identifying therapeutic targets, as the complex LD among ep-lets makes it statistically challenging to pinpoint the specific eplet truly driving the risk, distinguishing it from others that may appear significant due to strong LD.⁵⁵ Our analyses revealed that, while statistically significant ep-lets were significantly more likely to be so-called “antibody-verified” ep-lets (Figures S3A and S3B), ERS models derived using only the information from

antibody-verified eplets surprisingly performed worse than those derived using information from all eplets (Figures S3C and S3D), despite the expectation that antibody verification would enhance predictive performance.³³ Therefore, while eplets with large effect sizes driving *de novo* DSA development are often “antibody verified,” information from non-antibody-verified eplets also plays a significant role in enhancing prediction accuracy of the ERS. This finding implies that some genuine DSA-driving eplets may be hidden among the non-antibody-verified eplets⁵⁶ and that eplets with individually low DSA-driving risk can still play a critical role in refining DSA risk prediction, for example, through synergy with genuine DSA-driving eplets (likely to be “antibody verified”). Therefore, experimental verification efforts should ideally consider all relevant eplet mismatches comprehensively and, if possible, simultaneously. Given this, we acknowledge that, while our MLR results represent an important first step, they are not sufficient to adequately validate the hierarchy of eplet mismatches, necessitating further careful and rigorous experimental validation to establish a definitive hierarchy among eplet mismatches and to identify the genuine risk-driving eplets. Although this path is undoubtedly challenging, we remain optimistic that, through experimental validation, we can ultimately refine the ERS and identify therapeutic targets.

We have successfully identified and leveraged a previously unidentified hierarchy among mismatched HLA eplets in DSA development following organ transplantation, a principle that is universally applicable across various organ types. Our findings underscore the differential immunological significance of mismatched HLA eplets, thereby paving the way for optimized immunosuppressive strategies in organ transplantation and the development of therapeutics targeting highly immunogenic mismatched eplets.

Limitations of the study

First, we only focused on HLA class II eplets because the majority of DSAs target HLA class II. However, the impact of HLA class I eplets on clinical outcomes has also been reported and should be further explored.^{28,57} Second, in our study, we measured only HLA-DRB1 for HLA-DR and HLA-DQB1 for HLA-DQ due to current clinical practices in Japanese transplant settings, where routine testing is limited to HLA-A, HLA-B, HLA-C, HLA-DRB1, and HLA-DQB1. Our approach is partially justified by the following: (1) information from HLA-DRB1 allows us to impute HLA-DRB3/4/5 due to strong LD⁵⁸ and (2) the literature suggests that most DSAs against HLA-DQ target HLA-DQB1.⁵⁹ However, we acknowledged that, ideally, both HLA-DRB3/4/5 and HLA-DQA1 should be directly genotyped. For example, certain eplets are shared between the HLA-DRB3/4/5 and HLA-DRB1 loci. Consequently, without direct measurement, the misclassification of these eplets is sometimes unavoidable. Third, this study did not determine the specific eplets to which each detected DSA bound. Therefore, future studies that precisely identify the antigenic targets of DSAs are essential to confirm the immunogenicity of the DSA-associated eplets revealed by the machine learning approach in this study. Fourth, we only focused on B cell epitopes. However, the role of T cell epitopes is garnering interest, with current research seeking to estimate how HLA mis-

matches might act as T cell epitopes. Although experimental confirmation of T cell epitopes is presently sparse, incorporating their evaluation into future analyses is an intriguing prospect.⁶⁰ Fifth, we acknowledge that the potential impact of maintenance immunosuppression on the derivation of the ERS has not been fully accounted for. We believe that our approach of utilizing same-organ/same-center cohorts separately for the derivation and validation of the ERS minimizes the risk of the ERS being strongly influenced by differences in immunosuppressive protocols. In addition, adjustments for maintenance immunosuppression, based on the choice and number of immunosuppressive agents, did not alter the predictive ability of the ERS (Table S8). Nonetheless, we acknowledge that our study protocol and the variables used for may not fully account for the impact of the immunosuppressive regimen on the risk of DSA development. Other factors, such as drug handling, pharmacokinetics, pharmacodynamics, adherence, and clinical issues unrelated to rejection that necessitated immunosuppressant reductions—which were not quantified in this study—are also likely to play roles. Sixth, the limited number of events, particularly DR-DSA events in cohorts other than the pediatric living-donor liver transplant cohort, may lead to sparse-data bias, as evidenced by the unusually large HR estimates.⁶¹ Seventh, as HLA allele frequencies vary significantly among ethnic groups, the extrapolation of our results, obtained from a Japanese cohort, to other populations should be approached with caution.⁶² LD is one of the most significant sources of noise that complicates the estimation of the absolute risk of DSA for each eplet. Therefore, recruiting a relatively homogeneous Japanese population with a relatively consistent LD pattern undoubtedly significantly reduces noise caused by LD variability, enabling us to derive a highly predictive model even with a relatively small sample size (i.e., pediatric living-donor liver transplant cohort). However, in populations with different LD patterns, it is conceivable that the weights assigned to each eplet may change, raising uncertainty about whether the ERS model derived from the Japanese population can be directly applied to other populations. This challenge is similar to what has been observed in polygenic risk score (PRS) studies in population genetics.⁵⁵ Therefore, as in PRS research, the ultimate goal should be to develop models adaptable to multi-ancestry populations by increasing the sample size to a level that can overcome the noise introduced by LD variability across populations.⁵⁵ Eighth, we must acknowledge that, following internal validation in a small, older pediatric living-donor liver transplant cohort without pre-transplant anti-HLA antibody testing (Figures S1E, S2A, and S2B), standard external validation using pediatric living-donor liver transplant cohorts from external centers could not be conducted due to the unavailability of such cohorts. While we recognize this as an important limitation of our study, we wish to emphasize that, instead, validation was performed using cohorts that were understandably more challenging to validate. These included adult liver transplant cohorts and multi-organ transplant cohorts from both internal and external centers, encompassing a total of five cohorts: (1) adult living-donor liver transplant cohort, (2) living-donor lung transplant cohort, (3) deceased-donor lung transplant cohort, (4) living-donor kidney transplant cohort (Akita + Kyoto), and (5) older adult living-donor liver transplant

cohort. Finally, as this was a retrospective study involving two centers, our results should also be prospectively validated in a multicenter prospective cohort study.

RESOURCE AVAILABILITY

Lead contact

Requests for further information, resources, and reagents should be directed to and will be fulfilled by the lead contact, Dr. Takero Shindo (takeros@kuhp.kyoto-u.ac.jp).

Materials availability

An application capable of calculating ERS has been developed and deployed online (https://erscalculator.shinyapps.io/ers_application_deploy/).

Data and code availability

All raw flow cytometry data reported in this paper have been deposited in Mendeley Data: <https://doi.org/10.17632/6xbdr4f9nn.1>.

The codes used for statistical analyses have also been deposited in Mendeley Data: <https://doi.org/10.17632/6xbdr4f9nn.1>.

Any additional information required to reanalyze the data reported in this paper is available from the [lead contact](#) upon request.

ACKNOWLEDGMENTS

The authors would like to thank One Lambda, Inc. (a part of Thermo Fisher Scientific, Inc.) for all their support including providing anti-eplet monoclonal antibodies. The authors thank Terasaki Innovation Center, Inc. and Veritas Corporation for fruitful discussions relating to this study. A part of this study was conducted through the CORE Program of the Radiation Biology Center, Kyoto University. This work was supported by the Japan Agency for Medical Research and Development (grant number JP21ek0510035h0001-0003 to T.S.) and JSPS KAKENHI (grant numbers JP21J13724 to M.H., JP22K18178 to K.T., JP23K07811 to T.S., and JP21H02985 to S.Y.). The graphical abstract and [Figure 1](#) were created using a BioRender license.

AUTHOR CONTRIBUTIONS

M.H., K.T., and T.S. contributed to study design, data analysis, and manuscript drafting. M.H. and A. Kato performed the experimental analysis. K.T. primarily conducted statistical analysis. S.Y., T.I., S.T., M.S., and N.F. interpreted the clinical data and discussed the results. M.H., R.F., H.K., K.N., and N.F. contributed to data collection. K.Y. and R.H. contributed to the measurement of clinical samples. A. Kawaguchi supervised the statistical analysis. T.H., T.K., H.D., and E.H. supervised the study. All authors have read and approved the final version of this manuscript.

DECLARATION OF INTERESTS

The authors declare no competing interests.

STAR★METHODS

Detailed methods are provided in the online version of this paper and include the following:

- [KEY RESOURCES TABLE](#)
- [EXPERIMENTAL MODEL AND STUDY PARTICIPANT DETAILS](#)
 - Ethics statements
 - Cohort details
 - *In vitro* experiment
- [METHOD DETAILS](#)
 - HLA genotyping and HLA matching between donors and recipients at epitope level
 - Anti-HLA antibody testing and monitoring
 - Perioperative management and immunosuppression protocol

- Mixed lymphocyte reaction
- Production and verification of anti-eplet antibodies
- [QUANTIFICATION AND STATISTICAL ANALYSIS](#)

SUPPLEMENTAL INFORMATION

Supplemental information can be found online at <https://doi.org/10.1016/j.xcrm.2025.102153>.

Received: July 7, 2024

Revised: February 1, 2025

Accepted: May 2, 2025

Published: May 30, 2025

REFERENCES

1. Rodríguez-Perálvarez, M., Germani, G., Papastergiou, V., Tsochatzis, E., Thalassinou, E., Luong, T.V., Rolando, N., Dhillion, A.P., Patch, D., O'Beirne, J., et al. (2013). Early tacrolimus exposure after liver transplantation: relationship with moderate/severe acute rejection and long-term outcome. *J. Hepatol.* *58*, 262–270. <https://doi.org/10.1016/j.jhep.2012.09.019>.
2. Halloran, P.F., Chang, J., Famulski, K., Hidalgo, L.G., Salazar, I.D.R., Merino Lopez, M., Matas, A., Picton, M., de Freitas, D., Bromberg, J., et al. (2015). Disappearance of T Cell-Mediated Rejection Despite Continued Antibody-Mediated Rejection in Late Kidney Transplant Recipients. *J. Am. Soc. Nephrol.* *26*, 1711–1720. <https://doi.org/10.1681/ASN.2014060588>.
3. Loupy, A., and Lefaucheur, C. (2018). Antibody-Mediated Rejection of Solid-Organ Allografts. *N. Engl. J. Med.* *379*, 1150–1160. <https://doi.org/10.1056/NEJMra1802677>.
4. Valenzuela, N.M., and Reed, E.F. (2017). Antibody-mediated rejection across solid organ transplants: manifestations, mechanisms, and therapies. *J. Clin. Investig.* *127*, 2492–2504. <https://doi.org/10.1172/JCI90597>.
5. Lee, B.T., Fiel, M.I., and Schiano, T.D. (2021). Antibody-mediated rejection of the liver allograft: An update and a clinico-pathological perspective. *J. Hepatol.* *75*, 1203–1216. <https://doi.org/10.1016/j.jhep.2021.07.027>.
6. Levine, D.J., Glanville, A.R., Aboyou, C., Belperio, J., Benden, C., Berry, G.J., Hachem, R., Hayes, D., Neil, D., Reinsmoen, N.L., et al. (2016). Antibody-mediated rejection of the lung: A consensus report of the International Society for Heart and Lung Transplantation. *J. Heart. Lung. Transplant.* *35*, 397–406. <https://doi.org/10.1016/j.healun.2016.01.1223>.
7. Miyagawa-Hayashino, A., Yoshizawa, A., Uchida, Y., Egawa, H., Yurugi, K., Masuda, S., Minamiguchi, S., Maekawa, T., Uemoto, S., and Haga, H. (2012). Progressive graft fibrosis and donor-specific human leukocyte antigen antibodies in pediatric late liver allografts. *Liver Transpl.* *18*, 1333–1342. <https://doi.org/10.1002/lt.23534>.
8. Kaneku, H., O'Leary, J.G., Banuelos, N., Jennings, L.W., Susskind, B.M., Klintmalm, G.B., and Terasaki, P.I. (2013). De novo donor-specific HLA antibodies decrease patient and graft survival in liver transplant recipients. *Am. J. Transplant.* *13*, 1541–1548. <https://doi.org/10.1002/ajt.12212>.
9. Tikkanen, J.M., Singer, L.G., Kim, S.J., Li, Y., Binnie, M., Chaparro, C., Chow, C.-W., Martinu, T., Azad, S., Keshavjee, S., and Tinckam, K. (2016). De Novo DQ Donor-Specific Antibodies Are Associated with Chronic Lung Allograft Dysfunction after Lung Transplantation. *Am. J. Respir. Crit. Care Med.* *194*, 596–606. <https://doi.org/10.1164/rccm.201509-1857OC>.
10. Wiebe, C., Gibson, I.W., Blydt-Hansen, T.D., Karpinski, M., Ho, J., Storsley, L.J., Goldberg, A., Birk, P.E., Rush, D.N., and Nickerson, P.W. (2012). Evolution and clinical pathologic correlations of de novo donor-specific HLA antibody post kidney transplant. *Am. J. Transplant.* *12*, 1157–1167. <https://doi.org/10.1111/j.1600-6143.2012.04013.x>.

11. Devos, J.M., Gaber, A.O., Teeter, L.D., Graviss, E.A., Patel, S.J., Land, G. A., Moore, L.W., and Knight, R.J. (2014). Intermediate-term graft loss after renal transplantation is associated with both donor-specific antibody and acute rejection. *Transplantation* 97, 534–540. <https://doi.org/10.1097/01.TP.0000438196.30790.66>.
12. Terasaki, P.I., Ozawa, M., and Castro, R. (2007). Four-year follow-up of a prospective trial of HLA and MICA antibodies on kidney graft survival. *Am. J. Transplant.* 7, 408–415. <https://doi.org/10.1111/j.1600-6143.2006.01644.x>.
13. Gochi, F., Chen-Yoshikawa, T.F., Kayawake, H., Ohsumi, A., Tanaka, S., Yamada, Y., Yutaka, Y., Nakajima, D., Hamaji, M., Yurugi, K., et al. (2021). Comparison of de novo donor-specific antibodies between living and cadaveric lung transplantation. *J. Heart Lung Transplant.* 40, 607–613. <https://doi.org/10.1016/j.healun.2021.03.019>.
14. Robson, K.J., Ooi, J.D., Holdsworth, S.R., Rossjohn, J., and Kitching, A.R. (2018). HLA and kidney disease: from associations to mechanisms. *Nat. Rev. Nephrol.* 14, 636–655. <https://doi.org/10.1038/s41581-018-0057-8>.
15. Sheldon, S., and Poulton, K. (2006). HLA typing and its influence on organ transplantation. *Methods Mol. Biol.* 333, 157–174. <https://doi.org/10.1385/1-59745-049-9:157>.
16. Wiebe, C., Pochinco, D., Blydt-Hansen, T.D., Ho, J., Birk, P.E., Karpinski, M., Goldberg, A., Storsley, L.J., Gibson, I.W., Rush, D.N., and Nickerson, P.W. (2013). Class II HLA epitope matching-A strategy to minimize de novo donor-specific antibody development and improve outcomes. *Am. J. Transplant.* 13, 3114–3122. <https://doi.org/10.1111/ajt.12478>.
17. Wiebe, C., Rush, D.N., Nevins, T.E., Birk, P.E., Blydt-Hansen, T., Gibson, I. W., Goldberg, A., Ho, J., Karpinski, M., Pochinco, D., et al. (2017). Class II Eplet Mismatch Modulates Tacrolimus Trough Levels Required to Prevent Donor-Specific Antibody Development. *J. Am. Soc. Nephrol.* 28, 3353–3362. <https://doi.org/10.1681/ASN.2017030287>.
18. Mittal, K.K., and Terasaki, P.I. (1972). Cross-reactivity in the HL-A system. *Tissue Antigens* 2, 94–104. <https://doi.org/10.1111/j.1399-0039.1972.tb00123.x>.
19. Duquesnoy, R.J., and Schindler, T.E. (1976). Serological analysis of the HL-A10 complex. *Tissue Antigens* 7, 65–73. <https://doi.org/10.1111/j.1399-0039.1976.tb01034.x>.
20. Fuller, A.A., Trevithick, J.E., Rodey, G.E., Parham, P., and Fuller, T.C. (1990). Topographic map of the HLA-A2 CREG epitopes using human allo-antibody probes. *Hum. Immunol.* 28, 284–305. [https://doi.org/10.1016/0198-8859\(90\)90058-w](https://doi.org/10.1016/0198-8859(90)90058-w).
21. Rodey, G.E., Neylan, J.F., Whelchel, J.D., Revels, K.W., and Bray, R.A. (1994). Epitope specificity of HLA class I alloantibodies. I. Frequency analysis of antibodies to private versus public specificities in potential transplant recipients. *Hum. Immunol.* 39, 272–280. [https://doi.org/10.1016/0198-8859\(94\)90270-4](https://doi.org/10.1016/0198-8859(94)90270-4).
22. Park, M.S., Barbetti, A.A., Geer, L.I., Clark, B.D., Terasaki, P.I., and Aoki, J. (1990). HLA epitopes detected by serology. *Clin. Transpl.*, 515–531.
23. Tambur, A.R., and Claas, F.H.J. (2015). HLA epitopes as viewed by antibodies: what is it all about? *Am. J. Transplant.* 15, 1148–1154. <https://doi.org/10.1111/ajt.13192>.
24. El-Awar, N. (2022). HLA epitopes - Empirically defined as conformational amino acids sequences of the HLA antigen and are likely to be part of the binding sites of anti-HLA antibodies. *Hum. Immunol.* 83, 204–218. <https://doi.org/10.1016/j.humimm.2021.12.004>.
25. Duquesnoy, R.J. (2006). A structurally based approach to determine HLA compatibility at the humoral immune level. *Hum. Immunol.* 67, 847–862. <https://doi.org/10.1016/j.humimm.2006.08.001>.
26. Duquesnoy, R.J., Marrari, M., Tambur, A.R., Mulder, A., Sousa, L.C.D.d. M., da Silva, A.S., and do Monte, S.J.H. (2014). First report on the antibody verification of HLA-DR, HLA-DQ and HLA-DP epitopes recorded in the HLA Epitope Registry. *Hum. Immunol.* 75, 1097–1103. <https://doi.org/10.1016/j.humimm.2014.09.012>.
27. Bezstarosti, S., Bakker, K.H., Kramer, C.S.M., de Fijter, J.W., Reinders, M. E.J., Mulder, A., Claas, F.H.J., and Heidt, S. (2021). A Comprehensive Evaluation of the Antibody-Verified Status of Eplets Listed in the HLA Epitope Registry. *Front. Immunol.* 12, 800946. <https://doi.org/10.3389/fimmu.2021.800946>.
28. Kubal, C.A., Mangus, R., Ekser, B., Mihaylov, P., Ceballos, B., Higgins, N., Chalasani, N., Ghabril, M., Nephew, L., and Lobashevsky, A. (2018). Class II Human Leukocyte Antigen Epitope Mismatch Predicts De Novo Donor-Specific Antibody Formation After Liver Transplantation. *Liver Transpl.* 24, 1101–1108. <https://doi.org/10.1002/lt.25286>.
29. Walton, D.C., Cantwell, L., Hiho, S., Ta, J., Wright, S., Sullivan, L.C., Snell, G.I., and Westall, G.P. (2018). HLA class II Eplet mismatch predicts De Novo DSA formation post lung transplant. *Transpl. Immunol.* 51, 73–75. <https://doi.org/10.1016/j.trim.2018.10.002>.
30. Kramer, C.S.M., Franke-van Dijk, M.E.I., Bakker, K.H., Uyar-Mercankaya, M., Karahan, G.E., Roelen, D.L., Claas, F.H.J., and Heidt, S. (2020). Generation and reactivity analysis of human recombinant monoclonal antibodies directed against epitopes on HLA-DR. *Am. J. Transplant.* 20, 3341–3353. <https://doi.org/10.1111/ajt.15950>.
31. Hönger, G., Niemann, M., Schwalder, L., Jones, J., van Heck, M.R., van de Pasch, L.A.L., Vendelbosch, S., Rozemuller, E.H., Hösl, I., Blümel, S., and Schaub, S. (2020). Toward defining the immunogenicity of HLA epitopes: Impact of HLA class I eplets on antibody formation during pregnancy. *HLA* 96, 589–600. <https://doi.org/10.1111/tan.14054>.
32. McCaughan, J.A., Battle, R.K., Singh, S.K.S., Tikkanen, J.M., Moayed, Y., Ross, H.J., Singer, L.G., Keshavjee, S., and Tinckam, K.J. (2018). Identification of risk epitope mismatches associated with de novo donor-specific HLA antibody development in cardiothoracic transplantation. *Am. J. Transplant.* 18, 2924–2933. <https://doi.org/10.1111/ajt.14951>.
33. Sapir-Pichhadze, R., Zhang, X., Ferradji, A., Madbouly, A., Tinckam, K.J., Gebel, H.M., Blum, D., Marrari, M., Kim, S.J., Fingerson, S., et al. (2020). Epitopes as characterized by antibody-verified eplet mismatches determine risk of kidney transplant loss. *Kidney Int.* 97, 778–785. <https://doi.org/10.1016/j.kint.2019.10.028>.
34. Mohammadhassanzadeh, H., Oualkacha, K., Zhang, W., Klement, W., Bourdieu, A., Lamsatfi, J., Yi, Y., Foster, B., Keown, P., Gebel, H.M., et al. (2021). On Path to Informing Hierarchy of Eplet Mismatches as Determinants of Kidney Transplant Loss. *Kidney Int. Rep.* 6, 1567–1579. <https://doi.org/10.1016/j.ekir.2021.03.877>.
35. Williams, S.A., Kivimaki, M., Langenberg, C., Hingorani, A.D., Casas, J.P., Bouchard, C., Jonasson, C., Sarzynski, M.A., Shipley, M.J., Alexander, L., et al. (2019). Plasma protein patterns as comprehensive indicators of health. *Nat. Med.* 25, 1851–1857. <https://doi.org/10.1038/s41591-019-0665-2>.
36. Tsukita, K., Sakamaki-Tsukita, H., Kaiser, S., Zhang, L., Messa, M., Serrano-Fernandez, P., and Takahashi, R. (2023). High-Throughput CSF Proteomics and Machine Learning to Identify Proteomic Signatures for Parkinson Disease Development and Progression. *Neurology* 101, e1434–e1447. <https://doi.org/10.1212/WNL.0000000000207725>.
37. Riley, R.D., Ensor, J., Snell, K.I.E., Harrell, F.E., Martin, G.P., Reitsma, J.B., Moons, K.G.M., Collins, G., and van Smeden, M. (2020). Calculating the sample size required for developing a clinical prediction model. *BMJ* 368, m441. <https://doi.org/10.1136/bmj.m441>.
38. Boegel, S., Löwer, M., Bukur, T., Sorn, P., Castle, J.C., and Sahin, U. (2018). HLA and proteasome expression body map. *BMC Med. Genomics* 11, 36. <https://doi.org/10.1186/s12920-018-0354-x>.
39. Feng, S., Bucuvalas, J.C., Demetris, A.J., Burrell, B.E., Spain, K.M., Kanaparthi, S., Magee, J.C., Ikle, D., Lesniak, A., Lozano, J.J., et al. (2018). Evidence of Chronic Allograft Injury in Liver Biopsies From Long-term Pediatric Recipients of Liver Transplants. *Gastroenterology* 155, 1838–1851. e7. <https://doi.org/10.1053/j.gastro.2018.08.023>.
40. Goto, R., Fukasaku, Y., Ganchiku, Y., Kawamura, N., Watanabe, M., Ota, T., Hatanaka, K.C., Suzuki, T., Shimamura, T., and Taketomi, A. (2023). Post-transplant donor-specific anti-HLA antibodies with a higher mean

- fluorescence intensity are associated with graft fibrosis in pediatric living donor liver transplantation. *Front. Pediatr.* *11*, 1172516. <https://doi.org/10.3389/fped.2023.1172516>.
41. Takatsuki, M., Uemoto, S., Inomata, Y., Egawa, H., Kiuchi, T., Fujita, S., Hayashi, M., Kanematsu, T., and Tanaka, K. (2001). Weaning of immunosuppression in living donor liver transplant recipients. *Transplantation* *72*, 449–454. <https://doi.org/10.1097/00007890-200108150-00016>.
 42. Kulkarni, H.S., Bemiss, B.C., and Hachem, R.R. (2015). Antibody-mediated Rejection in Lung Transplantation. *Curr. Transplant. Rep.* *2*, 316–323. <https://doi.org/10.1007/s40472-015-0074-5>.
 43. Chen-Yoshikawa, T.F. (2021). Ischemia-Reperfusion Injury in Lung Transplantation. *Cells* *10*, 1333. <https://doi.org/10.3390/cells10061333>.
 44. Hamada, S., Dumortier, J., Thévenin, C., Pageaux, G.-P., Faure, S., Guillaud, O., Boillot, O., Lachaux, A., Luscalov, D.-A., Dubois, V., and Meszaros, M. (2020). Predictive value of HLA-Matchmaker and PIRCHE-II scores for de novo donor-specific antibody formation after adult and pediatric liver transplantation. *Transpl. Immunol.* *61*, 101306. <https://doi.org/10.1016/j.trim.2020.101306>.
 45. Tafulo, S., Malheiro, J., Santos, S., Dias, L., Almeida, M., Martins, L.S., Pedroso, S., Mendes, C., Lobato, L., and Castro-Henriques, A. (2021). HLA class II eplet mismatch load improves prediction of dnDSA development after living donor kidney transplantation. *Int. J. Immunogenet.* *48*, 1–7. <https://doi.org/10.1111/iji.12519>.
 46. Steele, D.J., Laufer, T.M., Smiley, S.T., Ando, Y., Grusby, M.J., Glimcher, L.H., and Auchincloss, H. (1996). Two levels of help for B cell alloantibody production. *J. Exp. Med.* *183*, 699–703. <https://doi.org/10.1084/jem.183.2.699>.
 47. Conlon, T.M., Saeb-Parsy, K., Cole, J.L., Motalebzadeh, R., Qureshi, M. S., Rehakova, S., Negus, M.C., Callaghan, C.J., Bolton, E.M., Bradley, J. A., and Pettigrew, G.J. (2012). Germinal center alloantibody responses are mediated exclusively by indirect-pathway CD4 T follicular helper cells. *J. Immunol.* *188*, 2643–2652. <https://doi.org/10.4049/jimmunol.1102830>.
 48. Siu, J.H.Y., Surendrakumar, V., Richards, J.A., and Pettigrew, G.J. (2018). T cell Allorecognition Pathways in Solid Organ Transplantation. *Front. Immunol.* *9*, 2548. <https://doi.org/10.3389/fimmu.2018.02548>.
 49. Dahdal, S., Saison, C., Valette, M., Bachy, E., Pallet, N., Lina, B., Koenig, A., Monneret, G., Defrance, T., Morelon, E., and Thauinat, O. (2018). Residual Activatability of Circulating Tfh17 Predicts Humoral Response to Thy-mo-dependent Antigens in Patients on Therapeutic Immunosuppression. *Front. Immunol.* *9*, 3178. <https://doi.org/10.3389/fimmu.2018.03178>.
 50. Marino, J., Babiker-Mohamed, M.H., Crosby-Bertorini, P., Paster, J.T., LeGuern, C., Germana, S., Abdi, R., Uehara, M., Kim, J.I., Markmann, J.F., et al. (2016). Donor exosomes rather than passenger leukocytes initiate alloreactive T cell responses after transplantation. *Sci. Immunol.* *1*, aaf8759. <https://doi.org/10.1126/sciimmunol.aaf8759>.
 51. Hughes, A.D., Zhao, D., Dai, H., Abou-Daya, K.I., Tieu, R., Rammal, R., Williams, A.L., Landsittel, D.P., Shlomchik, W.D., Morelli, A.E., et al. (2020). Cross-dressed dendritic cells sustain effector T cell responses in islet and kidney allografts. *J. Clin. Investig.* *130*, 287–294. <https://doi.org/10.1172/JCI125773>.
 52. Harper, I.G., Ali, J.M., Harper, S.J.F., Wlodek, E., Alsughayyir, J., Negus, M.C., Qureshi, M.S., Motaleb-Zadeh, R., Saeb-Parsy, K., Bolton, E.M., et al. (2016). Augmentation of Recipient Adaptive Alloimmunity by Donor Passenger Lymphocytes within the Transplant. *Cell Rep.* *15*, 1214–1227. <https://doi.org/10.1016/j.celrep.2016.04.009>.
 53. Charmentant, X., Chen, C.-C., Hamada, S., Goncalves, D., Saison, C., Rabeyrin, M., Rabant, M., Duong van Huyen, J.-P., Koenig, A., Mathias, V., et al. (2022). Inverted direct allorecognition triggers early donor-specific antibody responses after transplantation. *Sci. Transl. Med.* *14*, eabg1046. <https://doi.org/10.1126/scitranslmed.abg1046>.
 54. Iwahara, N., Hotta, K., Iwami, D., Tanabe, T., Tanaka, Y., Ito, Y.M., Otsuka, T., Murai, S., Takada, Y., Higuchi, H., et al. (2023). Analysis of T-cell allo-antigen response via a direct pathway in kidney transplant recipients with donor-specific antibodies. *Front. Immunol.* *14*, 1164794. <https://doi.org/10.3389/fimmu.2023.1164794>.
 55. Martin, A.R., Kanai, M., Kamatani, Y., Okada, Y., Neale, B.M., and Daly, M. J. (2019). Clinical use of current polygenic risk scores may exacerbate health disparities. *Nat. Genet.* *51*, 584–591. <https://doi.org/10.1038/s41588-019-0379-x>.
 56. Heidt, S., and Claas, F.H.J. (2020). Not all HLA epitope mismatches are equal. *Kidney Int.* *97*, 653–655. <https://doi.org/10.1016/j.kint.2019.12.017>.
 57. Haririan, A., Fagoaga, O., Daneshvar, H., Morawski, K., Sillix, D.H., El-Amm, J.M., West, M.S., Garnick, J., Migdal, S.D., Gruber, S.A., and Nehlsen-Cannarella, S. (2006). Predictive value of human leucocyte antigen epitope matching using HLA-Matchmaker for graft outcomes in a predominantly African-American renal transplant cohort. *Clin. Transplant.* *20*, 226–233. <https://doi.org/10.1111/j.1399-0012.2005.00473.x>.
 58. Nakajima, F., Nakamura, J., and Yokota, T. (2001). Analysis of HLA haplotypes in Japanese, using high resolution allele typing. *MHC* *8*, 1–32. <https://doi.org/10.12667/mhc.8.1>.
 59. Tagliamacco, A., Cioni, M., Comoli, P., Ramondetta, M., Brambilla, C., Trivelli, A., Magnasco, A., Bitocchi, R., Fontana, I., Dulbecco, P., et al. (2014). DQ molecules are the principal stimulators of de novo donor-specific antibodies in nonsensitized pediatric recipients receiving a first kidney transplant. *Transpl. Int.* *27*, 667–673. <https://doi.org/10.1111/tri.12316>.
 60. Otten, H.G., Calis, J.J.A., Keşmir, C., van Zuilen, A.D., and Spierings, E. (2013). Predicted indirectly recognizable HLA epitopes presented by HLA-DR correlate with the de novo development of donor-specific HLA IgG antibodies after kidney transplantation. *Hum. Immunol.* *74*, 290–296. <https://doi.org/10.1016/j.humimm.2012.12.004>.
 61. Greenland, S., Mansournia, M.A., and Altman, D.G. (2016). Sparse data bias: a problem hiding in plain sight. *BMJ* *352*, i1981. <https://doi.org/10.1136/bmj.i1981>.
 62. Dasariraju, S., Gragert, L., Wager, G.L., McCullough, K., Brown, N.K., Kammoun, M., and Urbanowicz, R.J. (2023). HLA amino acid Mismatch-Based risk stratification of kidney allograft failure using a novel Machine learning algorithm. *J. Biomed. Inform.* *142*, 104374. <https://doi.org/10.1016/j.jbi.2023.104374>.
 63. Jatana, S.S., Zhao, H., Bow, L.M., Cozzi, E., Batal, I., Horak, T., Amar-Zifkin, A., Schinstock, C., Askar, M., Dadhania, D.M., et al. (2023). Seeking Standardized Definitions for HLA-incompatible Kidney Transplants: A Systematic Review. *Transplantation* *107*, 231–253. <https://doi.org/10.1097/TP.0000000000004262>.
 64. Duquesnoy, R.J., and Askar, M. (2007). HLA-Matchmaker: a molecularly based algorithm for histocompatibility determination. V. Eplet matching for HLA-DR, HLA-DQ, and HLA-DP. *Hum. Immunol. Ser.* *68*, 12–25. <https://doi.org/10.1016/j.humimm.2006.10.003>.
 65. Hirata, M., Yagi, S., Shindo, T., Yoshizawa, A., Kiguchi, G., Kaneshiro, M., Yurugi, K., Miyachi, Y., Iwamura, S., Yao, S., and Uemoto, S. (2021). Donor-dominant one-way matching of human leukocyte antigen-A/B/DR alleles predicts graft-versus-host disease following living donor liver transplantation. *Hepatol. Res.* *51*, 135–148. <https://doi.org/10.1111/hepr.13579>.
 66. Date, H., Sato, M., Aoyama, A., Yamada, T., Mizota, T., Kinoshita, H., Handa, T., Tanizawa, K., Chin, K., Minakata, K., and Chen, F. (2015). Living-donor lobar lung transplantation provides similar survival to cadaveric lung transplantation even for very ill patients. *Eur. J. Cardio. Thorac. Surg.* *47*, 967–973, discussion 972–973. <https://doi.org/10.1093/ejcts/ezu350>.
 67. Kobayashi, T., Nakamoto, Y., Sunada, T., Sawada, A., Yamasaki, T., and Ogawa, O. (2020). ^{99m}Tc-mercaptoacetyltriglycine Cortical Renography Predicts Outcomes in Adult Living Donor Renal Transplant Recipients. *Transplant. Proc.* *52*, 3090–3096. <https://doi.org/10.1016/j.transproceed.2020.02.169>.
 68. Inoue, T., Saito, M., Narita, S., Numakura, K., Tsuruta, H., Maeno, A., Tsuchiya, N., Satoh, S., and Habuchi, T. (2017). Evaluation of Persistent Lymphatic Fluid Leakage Using a Strategy of Placing a Drain After Kidney

- Transplantation: A Statistical Analysis to Assess Its Origin. *Transplant. Proc.* 49, 1786–1790. <https://doi.org/10.1016/j.transproceed.2017.06.021>.
69. Fujiyama, N., Satoh, S., Saito, M., Numakura, K., Inoue, T., Yamamoto, R., Saito, T., Kanda, S., Narita, S., Mitobe, Y., and Habuchi, T. (2019). Impact of persistent preformed and de novo donor-specific antibodies detected at 1 year after kidney transplantation on long-term graft survival in Japan: a retrospective study. *Clin. Exp. Nephrol.* 23, 1398–1406. <https://doi.org/10.1007/s10157-019-01780-z>.
70. Loupy, A., Haas, M., Roufosse, C., Naesens, M., Adam, B., Afrouzian, M., Akalin, E., Alachkar, N., Bagnasco, S., Becker, J.U., et al. (2020). The Banff 2019 Kidney Meeting Report (I): Updates on and clarification of criteria for T cell- and antibody-mediated rejection. *Am. J. Transplant.* 20, 2318–2331. <https://doi.org/10.1111/ajt.15898>.
71. Solez, K., Axelsen, R.A., Benediktsson, H., Burdick, J.F., Cohen, A.H., Colvin, R.B., Croker, B.P., Droz, D., Dunnill, M.S., and Halloran, P.F. (1993). International standardization of criteria for the histologic diagnosis of renal allograft rejection: the Banff working classification of kidney transplant pathology. *Kidney Int.* 44, 411–422. <https://doi.org/10.1038/ki.1993.259>.
72. Demetris, A.J., Bellamy, C., Hübscher, S.G., O'Leary, J., Randhawa, P.S., Feng, S., Neil, D., Colvin, R.B., McCaughan, G., Fung, J.J., et al. (2016). 2016 Comprehensive Update of the Banff Working Group on Liver Allograft Pathology: Introduction of Antibody-Mediated Rejection. *Am. J. Transplant.* 16, 2816–2835. <https://doi.org/10.1111/ajt.13909>.
73. Demetris, A., Adams, D., Bellamy, C., Blakolmer, K., Clouston, A., Dhillon, A.P., Fung, J., Gouw, A., Gustafsson, B., Haga, H., et al. (2000). Update of the International Banff Schema for Liver Allograft Rejection: working recommendations for the histopathologic staging and reporting of chronic rejection. An International Panel. *Hepatology* 31, 792–799. <https://doi.org/10.1002/hep.510310337>.
74. Shindo, T., Kim, T.K., Benjamin, C.L., Wieder, E.D., Levy, R.B., and Komanduri, K.V. (2013). MEK inhibitors selectively suppress alloreactivity and graft-versus-host disease in a memory stage-dependent manner. *Blood* 121, 4617–4626. <https://doi.org/10.1182/blood-2012-12-476218>.
75. Deng, C.-T., Cai, J., Tarsitani, C., El-Awar, N., Lachmann, N., and Ozawa, M. (2006). HLA class II DQ epitopes. *Clin. Transpl.*, 115–122.
76. Deng, C.-T., El-Awar, N., Ozawa, M., Cai, J., Lachmann, N., and Terasaki, P.I. (2008). Human leukocyte antigen class II DQ alpha and beta epitopes identified from sera of kidney allograft recipients. *Transplantation* 86, 452–459. <https://doi.org/10.1097/TP.0b013e3181804cd2>.

STAR★METHODS

KEY RESOURCES TABLE

REAGENT or RESOURCE	SOURCE	IDENTIFIER
Antibodies		
Anti-CD4 PE-Cy7 antibody (clone SK3)	Becton, Dickinson and Company	Cat#348789; RRID:AB_400379
Anti-CD8a PerCP-Cy5.5 antibody (clone RPA-T8)	Biolegend	Cat#301032; RRID:AB_893422
Mouse monoclonal IgM antibodies against HLA-DQB1	Thermo Fisher Scientific (One Lambda)	N/A
Biological samples		
Peripheral blood mononuclear cells	Healthy volunteers	N/A
Chemicals, peptides, and recombinant proteins		
CFSE	Thermo Fisher Scientific	Cat#C34554
RPMI 1640	Nacalai Tesque	Cat#30264-56
Critical commercial assays		
WAKFlow HLA Typing kit	Wakunaga Pharmaceutical Co. Ltd.	N/A
Luminex xMAP Technology	Luminex Corporation	N/A
Pierce IgM Purification Kit	Thermo Fisher Scientific	Cat#44897
LABType™ SSO	Thermo Fisher Scientific (One Lambda)	Cat#RSSO1A
LABScreen Mixed	Thermo Fisher Scientific (One Lambda)	Cat#LSM12
LABScreen PRA	Thermo Fisher Scientific (One Lambda)	Cat#LS1PRA
LABScreen Single Antigen	Thermo Fisher Scientific (One Lambda)	Cat#LSA1A04
Deposited data		
Raw flow cytometry data and R scripts	This paper	https://doi.org/10.17632/6xbdr4f9nn.1
ERS calculation application	This paper	https://erscalculator.shinyapps.io/ers_application_deploy/
Software and algorithms		
HLA Matchmaker Class I/II Reference File 2017.08	Thermo Fisher Scientific (One Lambda)	https://www.thermofisher.com/onelambda/us/en/home.html
FACSLyric	Becton, Dickinson and Company	N/A
FlowJo software	Becton, Dickinson and Company	RRID:SCR_008520
One Lambda Incorporated Fusion Matchmaker software, version 4.4	Thermo Fisher Scientific (One Lambda)	https://www.thermofisher.com/onelambda/us/en/home.html (Cat# FUSPGR)
R, version 4.0.5	The R foundation	https://www.r-project.org/ ; RRID:SCR_001905
survival R package, version 3.4.0	The R foundation	https://cran.r-project.org/package=survival ; RRID:SCR_021137
weights R package, version 1.0.4	The R foundation	https://CRAN.R-project.org/package=weights
glmnet R package, version 4.1.4	The R foundation	https://cran.r-project.org/package=glmnet
ppcor R package, version 1.1	The R foundation	https://cran.r-project.org/package=ppcor
BioRender	BioRender	https://www.biorender.com/

EXPERIMENTAL MODEL AND STUDY PARTICIPANT DETAILS

Ethics statements

This study was approved by the Institutional Review Board of Kyoto University (R2584-4 and G0697) and was performed in accordance with the institutional guidelines and the Declaration of Helsinki. The use of deceased-donor data in this study was requested to Japan Organ Transplant Network (JOT), and was approved by the Institutional Review Board in JOT.

Cohort details

This retrospective study encompassed six distinct cohorts of liver, lung, and kidney transplantations from two Japanese transplant centers (Kyoto University Hospital and Akita University Hospital). Patients who did not meet the exclusion criteria (as detailed below) were consecutively enrolled within the specified study period. For liver transplantation, two cohorts from Kyoto University Hospital (total $n = 592$) were used, comprising pediatric cases (recipient age at transplant <18 years) and adult cases (≥ 18 years), who all received transplants from living donors. For lung transplantation, two cohorts from Kyoto University Hospital (total $n = 276$) were used, consisting of cases from living donors and cases from deceased donors. As for kidney transplantation, two cohorts were used, one from Kyoto University Hospital ($n = 69$) and the other from Akita University Hospital ($n = 428$). The following exclusion criteria were applied to all cohorts: transplants that had no allele-level HLA typing data, had preformed DSA, and had no pre- or post-transplant anti-HLA antibody test data. As a note, re-transplant cases were not excluded from the study because, although they involve the same recipient, each represents a unique donor-recipient pair with distinct eplet mismatch profiles.

Finally, this study included 173 cases of pediatric living-donor liver transplantation and 159 cases of adult living-donor liver transplantation, out of a total of 517 cases (including 207 pediatrics and 310 adults) performed at Kyoto University Hospital between January 2010 and February 2022. Liver transplant recipient follow-up was censored at March 1, 2022. Additionally, this study enrolled 97 cases of living-donor lobar lung transplantation and 151 cases of deceased-donor lung transplantation out of 276 cases of lung transplantation (including 104 cases from living donors and 173 cases from deceased donors) performed at Kyoto University Hospital between January 2010 and February 2022. One case who received a hybrid lung transplant using grafts from a deceased donor and a living donor was placed in both the living- and deceased-donor cohorts according to the graft origin. Among the 97 living-donor lung transplant cases, 85 cases received lung grafts from two different donors, resulting in 182 donor-recipient pairs. Lung transplant recipient follow-up was also censored at March 1, 2022. Furthermore, this study included 266 cases out of 414 cases of living-donor kidney transplantation performed at Akita University Hospital between February 1998 and June 2022. Additionally, 47 cases were enrolled out of 53 cases of living-donor kidney transplantation performed at Kyoto University Hospital between January 2010 and February 2022. Kidney recipient follow-up was censored at December 31, 2022.

Moreover, two independent additional cohorts of pediatric and adult living-donor liver transplantation performed at Kyoto University Hospital in an earlier era (total $n = 1437$), preceding the original cohort, were used to validate the established model. Among the 1,420 cases of living-donor liver transplantation performed between June 1990 and December 2009, 38 pediatric and 26 adult cases were included after excluding transplants that had no allele-level HLA typing data and had no post-transplant anti-HLA antibody test data. This cohort included recipients who did not undergo pre-transplant anti-HLA antibody testing. The recipient follow-up was censored at December 31, 2022. The age and gender of the study participants are summarized in [Table S1](#). The cohort consisted of 99.8% Japanese individuals. Gender was not found to be associated with the outcomes of this study.

As an additional note, the physicians who conducted the follow-up for each cohort were different from those who collected the data and those who analyzed it. The results of the evaluation of our datasets and analyses in relation to the recommendations outlined by the Banff Antibody-Mediated Injury Working Group are presented in [Table S11](#).⁶³

In vitro experiment

PBMCs were isolated from six randomly selected healthy volunteers. All donors were Japanese, and their age and gender are summarized in [Table S9](#). Using these PBMCs, a total of 11 random donor-recipient pairs were generated, and MLR assays were performed.

METHOD DETAILS

HLA genotyping and HLA matching between donors and recipients at epitope level

Allele-level genotyping of HLA-A, -B, -C, -DRB1, and -DQB1 was performed by PCR, using sequence-specific oligonucleotide probes, the WAKFlow HLA Typing kit (Wakunaga Pharmaceutical Co. Ltd.), and Luminex xMAP Technology (Luminex Corporation). LABType SSO (One Lambda, Inc.) was also used at Akita University Hospital. HLA incompatibility (in the rejection direction) between donors and recipients at epitope level was evaluated following allele-level HLA typing using the One Lambda Incorporated Fusion Matchmaker software (v4.4).⁶⁴ The list of eplets was provided by One Lambda as an HLA Matchmaker Class I/II Reference File 2017.08 (<https://www.thermofisher.com/onelambda/us/en/home.html>), based on data from the HLA Eplet Registry (<https://www.epregistry.com.br>). All eplets, including antibody-verified eplets, were used for analysis. The HLA-DRB1 and HLA-DQB1 mismatched eplets were highlighted, in addition to the number of eplet mismatches at each HLA locus. In transplants that involved two donors, such as some of the living-donor lung transplants, HLA incompatibility between each donor-recipient pair was evaluated. Some of

lung transplant recipients previously received allogeneic hematopoietic stem cell transplantation. Their HLA genotyping was performed after hematopoietic stem cell transplantation but before lung transplantation, which reflected hematopoietic stem cell transplantation donors' genotypes.

Anti-HLA antibody testing and monitoring

Regarding serum handling and DSA assignments, we made every effort to ensure consistency across organs and centers. Importantly, both institutions (Kyoto University Hospital and Akita University Hospital) participate in a quality control workshop organized by the Japanese Society for Histocompatibility and Immunogenetics (<https://jshi.smoosy.atlas.jp/ja>) and are certified for reliable histocompatibility testing, including HLA typing and anti-HLA antibody assays. In this study, antibodies against HLA-A, -B, -C, -DRB1/3/4/5, and -DQB1 were screened periodically using LABScreen Mixed (One Lambda, Inc.) at Kyoto University Hospital and LABScreen PRA at Akita University Hospital, respectively. When anti-HLA antibodies were detected, their specificities were identified using the LABScreen Single Antigen (One Lambda, Inc.) at both institutions. The DSA result was considered positive when the normalized mean fluorescence intensity was more than 1,000. In this study, we focused on the DSA against HLA Class II. For DSA against HLA-DR (DR-DSA), the associations between DSA against HLA-DRB1/3/4/5 and HLA-DRB1 eplet mismatches were evaluated. Meanwhile, for DSA against HLA-DQ (DQ-DSA), the associations between DSA against HLA-DQB1 and HLA-DQB1 eplet mismatches were evaluated. We utilized the HLA Fusion Matchmaker software, a tool that identifies eplet mismatches by processing information pertaining to each HLA allele of the donor and recipient. This software allowed us to extract information about 142 DRB1 and 60 DQB1 independent eplets. Because our cohorts predominantly comprised Japanese donors and recipients (99.8%), the DSA against untyped HLA-DRB3/4/5 was determined based on its robust linkage on allele level with HLA-DRB1 (97.7%) within the haplotype of a Japanese population.⁵⁸ We assumed that, due to this strong linkage disequilibrium, the development of DSA against HLA-DRB3/4/5 could also be predicted by HLA-DRB1 eplet mismatches. DSA against HLA-DQA1 was not screened because the majority of DSA against HLA-DQ target HLA-DQB1.⁵⁹ The DSA was routinely measured preoperatively and was checked annually after transplantation, in addition to when the recipient presented with symptoms or had abnormal findings. Specifically, within one year after lung transplantation, screening was routinely performed 1 week, 1 month, 3 months, and 6 months after transplantation. In cases of kidney transplantation performed at Akita University Hospital prior to the initiation of anti-HLA antibody testing in 2014, the presence of DSA was examined through the analysis of collected and stored serum samples.

Perioperative management and immunosuppression protocol

The selection criteria for donors and recipients, the surgical procedures, and the immunosuppression regimens employed have been previously described in detail.^{7,13,65–69} For the selection criteria, living donors were selected from immediate family members.

As for the immunosuppression regimens, in pediatric liver transplantation, tacrolimus (TAC) and steroids were used as the standard immunosuppressive regimen without induction therapy. TAC was administered immediately after transplantation, with a target trough level of 10–12 ng/mL for the first two weeks, 8–10 ng/mL for the first month, 6–8 ng/mL for the first year, and 4–6 ng/mL thereafter. Steroids, administered as methylprednisolone at 10 mg/kg intravenously during surgery before graft reperfusion, were continued postoperatively and tapered until discontinuation after three months. Mycophenolate mofetil (MMF) was added at a dose of 10–20 mg/kg as needed, typically in response to rejection episodes. In adult liver transplantation, TAC and MMF comprised the standard immunosuppressive regimen, with steroids limited to a single intraoperative dose of methylprednisolone at 10 mg/kg, and induction therapy was not used. TAC administration protocol was consistent with that used in pediatric cases. MMF was initiated post-transplant at 1,000–2,000 mg/day and reduced to 500–1,000 mg/day after three months for maintenance. For recipients with autoimmune-related liver diseases, steroids were continued postoperatively at 2.5–5 mg/day beyond three months. Recently, in cases with renal impairment, everolimus (EVR) was added one month post-transplant to reduce TAC dosing, with target trough levels set at 3–8 ng/mL for EVR and 4–6 ng/mL for TAC. For adult cases prior to January 2011, TAC and low-dose steroids were the standard immunosuppressive regimen, with MMF added in cases of steroid-resistant rejection or when side effects from TAC occurred. In ABO-incompatible cases, rituximab was administered 2–3 weeks before transplantation at a dose of 375 mg/m² for pediatric patients aged two years and older, and 500 mg/body for adults. TAC (target trough level 3–5 ng/mL) and MMF (1,000 mg/day for adults and 10 mg/kg/day for pediatric patients) were started one week before transplantation. Plasma exchange or exchange transfusion (in pediatric cases) was performed as needed. Post-transplant, steroids were continued following intraoperative administration and tapered until discontinued after six months.

In lung transplantation, a standard immunosuppressive regimen consisting of TAC, MMF (or azathioprine), and steroids was used, without induction therapy. TAC was administered immediately post-transplant, with a target trough level of 10–15 ng/mL maintained for the first six months, then reduced to 8–10 ng/mL thereafter. MMF was started immediately post-transplant at 1,000–1,500 mg/day and continued at this dose. If azathioprine was used, it was initiated post-transplant at 2 mg/kg and maintained at this dosage. For steroids, methylprednisolone was administered intraoperatively at 500 mg for adult patients and 125 mg for pediatric patients intravenously before graft reperfusion, followed by continued use post-transplant at a dose of 0.4 mg/kg/day for the first six months, then tapered to 0.1 mg/kg/day. The immunosuppressant protocol was the same for both deceased-donor and living-donor lung transplants.

In kidney transplantation at Kyoto University Hospital, a standard immunosuppressive regimen of TAC, MMF, and steroids was used. Basiliximab was administered as induction therapy at a dose of 20 mg/body intravenously immediately post-transplant and

on day four post-transplant. TAC was started 3–5 days before transplantation, with a target trough level of 8–12 ng/mL maintained for the first month, 7–9 ng/mL for up to three months post-transplant, and 4–6 ng/mL thereafter. MMF was also initiated 3–5 days pre-operatively at 2,000 mg/day and continued at this dose post-transplant. For steroids, methylprednisolone was administered at 500 mg intravenously during surgery before graft reperfusion and was subsequently tapered to 5 mg/day, which was maintained beyond three months post-transplant. In ABO-incompatible cases, rituximab was administered at 200 mg/body two weeks prior to transplantation. Additionally, TAC (target trough 8–12 ng/mL), MMF (2,000 mg/day), and prednisone (25 mg/day) were initiated three weeks prior to transplantation. Double-filtration plasmapheresis (DFPP) was performed three times on alternate days, with plasma exchange conducted on the day before surgery. At Akita University Hospital, a standard immunosuppressive regimen of TAC, MMF, steroids, and EVR was used. Basiliximab administered as induction therapy was consistent with the protocol used at Kyoto University. TAC was started two days before transplantation, with a target trough level of 10–12 ng/mL for the first week, 8–10 ng/mL for the second week, and 8 ng/mL for the first month, then adjusted to 5–8 ng/mL, and finally reduced to a maintenance level of 4 ng/mL. MMF was initiated at 1,500 mg/day two days before transplantation, then reduced to 1,000 mg/day after two weeks post-transplant and continued. Methylprednisolone was administered at 500 mg intravenously during surgery before graft reperfusion and gradually tapered to 10 mg/day by one month post-transplant. For patients with chronic glomerulonephritis or autoimmune-related diseases, steroids were continued at 5 mg/day, while in patients with diabetic nephropathy, nephrosclerosis, autosomal dominant polycystic kidney disease (ADPKD), or reflux nephropathy, steroids were discontinued by six months post-transplant. EVR was introduced two weeks after transplantation with a target trough level of 3–5 ng/mL and maintained at this level. In ABO-incompatible cases, rituximab was administered at a dose of 200 mg/body three weeks prior to transplantation. MMF (1,500 mg/day) was started three weeks before transplantation, while TAC (target trough 10–12 ng/mL) and prednisone (80 mg/day) were initiated one week before transplantation. DFPP and plasma exchange were performed as necessary based on antibody titers. In cases of any organ transplant where discontinuation of TAC was required due to side effects such as encephalopathy, cyclosporine was used as an alternative.

Acute rejection in liver and kidney transplants was diagnosed histopathologically according to the Banff criteria.^{70–73} In liver transplants, for-cause biopsies were performed in response to clinical findings such as deteriorating graft liver function or increasing ascites. Protocol biopsies were conducted 3–5 years post-transplant, or 2–3 years post-transplant in recipients with autoimmune-related liver diseases. Follow-up biopsies were performed 3–6 months after immunosuppressive dose reduction or 3–5 years post-transplant in DSA-positive recipients. In kidney transplants, for-cause biopsies were performed in response to clinical findings such as elevated creatinine, proteinuria, or the emergence of *de novo* DSA. Regarding protocol biopsies, Kyoto University Hospital conducted them at 3 months, 1 year, and 3 years post-transplant, while Akita University Hospital conducted them at 1 month, 6 months, and 1 year post-transplant. Additionally, at Kyoto University Hospital, follow-up biopsies were performed 6 to 12 months after the previous biopsy in cases diagnosed with rejection, including those with borderline changes. In lung transplants, acute rejection was diagnosed clinically considering patients' symptom, blood test, bacterial culture test of the sputum, bronchoscopic findings, and radiological findings. AMR, specifically cases classified as "clinical possible AMR," was diagnosed according to the criteria outlined in the consensus report of the International Society for Heart and Lung Transplantation.⁶ Across all organ cohorts, steroid pulse therapy was employed as the first-line treatment for rejection events. For steroid-resistant rejection, antithymocyte globulin was considered depending on the clinical context. In cases of AMR, intravenous immunoglobulin, plasmapheresis, and rituximab were administered as appropriate, based on the specific clinical presentation of each case.

Mixed lymphocyte reaction

PBMCs were collected from six healthy volunteers with genotyped HLA alleles, following written informed consent (Table S9). Using these PBMCs, 11 stimulator-responder pairs were then randomly formed, and their total ERS were calculated by adding DR-ERS and DQ-ERS (Table S9). A mixed lymphocyte reaction (MLR) was then performed using the CFSE labeling technique for evaluating immune responses to alloantigens.⁷⁴ PBMCs were isolated by Ficoll-Hypaque density gradient sedimentation using Lympholyte-H (Cedarlane Laboratories). 5 μ M CFSE (Thermo Fisher Scientific, C34554) was used to label responder PBMCs, which were then co-cultured with 20 Gy-irradiated allogeneic stimulator PBMCs in 200 μ L of RPMI 1640 (Nacalai Tesque) supplemented with 10% human AB serum (Sigma-Aldrich, H4522) in 96-well round bottom plates for 5 days. The stimulator and responder cells (each suspended in 100 μ L media) were then co-incubated in a 1:1 ratio, and the cell density was adjusted to 0.5×10^6 cells per well. T cell activation status was assessed using flow cytometry by measuring cell division as dilution of CFSE. Flow cytometric analysis was performed using the anti-CD4 phycoerythrin-cyanin 7 (PE-Cy7; clone SK3, Becton, Dickinson and Company) and anti-CD8a peridinin chlorophyll protein-cyanin 5.5 (PerCP-Cy5.5; clone RPA-T8, Biolegend) antibodies. Samples were acquired on the FACSLytic (Becton, Dickinson and Company) flow cytometer and analyzed using FlowJo software (Becton, Dickinson and Company). A minimum of three MLR experiments were performed for each stimulator-responder pair. The correlations between total ERS and the percentage of CFSE^{low} CD4⁺ and CD8⁺ T cells were then analyzed.

Production and verification of anti-eplet antibodies

Two mouse monoclonal IgM antibodies against HLA-DQB1 molecules, generated by hybridoma technology, were kindly provided by One Lambda. The reactivity of these antibodies against eplets was verified using One Lambda Incorporated Fusion Matchmaker software through LABScreen Single Antigen (One Lambda, Inc.). One anti-HLA-DQ7/8/9 antibody was specific for the 55PP eplet,

whereas the other anti-HLA-DQ7 antibody targeted the 45EV eplet.^{75,76} The two IgM antibodies were supplied within frozen mouse ascites and were subsequently purified using the Pierce IgM Purification Kit (Thermo Fisher Scientific, #44897). The purified IgM antibodies were stored at -20°C in glycerol. PBMCs from one pair of HLA-mismatched healthy volunteers (pair #4; Table S9), in which the 55PP eplet was mismatched on HLA-DQB1, were selected as stimulators and responders in the MLR. The 45EV eplet was not present on any of the HLA alleles belonging to this pair of PBMC donors. The two IgM antibodies were added to the wells containing irradiated stimulator PBMCs at the following concentrations: 1×10^1 ng/mL, 1×10^2 ng/mL, or 1×10^3 ng/mL. After 30 min, the CFSE-labeled responder PBMCs were added, and the cells were cocultured for 5 days. The percentages of CFSE^{low} CD4⁺ and CD8⁺ T cells were assessed by flow cytometry.

QUANTIFICATION AND STATISTICAL ANALYSIS

From the 142 HLA-DRB1 and 60 HLA-DQB1 eplets listed within the One Lambda Incorporated Fusion Matchmaker software, data on mismatched eplets detected in individuals who had developed DSA were extracted. Within our cohort, 105 DRB1 and 55 DQB1 eplets were identified as mismatched at least once in patients who developed DSA. To assess eplet clustering, we calculated the JI between each pair of these eplets. Specifically, the number of cases in which two specific eplets were detected as mismatched together was divided by the number of cases in which at least one of these two eplets was detected as mismatched. Subsequently, based on the Jaccard distance (i.e., $1 - \text{JI}$), hierarchical clustering was performed using the “hclust()” function of the “stats” R package (version 4.2.1), specifying “ward.D2” as the clustering method (<https://www.R-project.org/>). To visualize this intricate eplet relatedness, we used dendrograms coupled with triangular matrices. For instance, in the case of DRB1 eplets, a mismatched 181M eplet always coincided with a mismatched 181VMP eplet, as indicated by a JI of 1.0. Eplets 4Q, 78V2, 30G, 13FEY, and 28H were also frequently identified as mismatched eplets, showing JI values of 0.98, 0.98, 0.91, 0.91, and 0.91, respectively. This illustrates a strong tendency for these eplets to be simultaneously mismatched.

To prioritize important eplets in the subsequent DSA development, the effect of each mismatched eplet on time to DSA development was estimated using a Cox proportional hazards model, with age and gender as covariates. This analysis was primarily conducted using the “coxph()” and “Surv()” functions of the “survival” R package (version 3.4.0). Statistical significance was assessed by testing the null hypothesis that the β coefficients equaled zero using the Wald test. Multiple testing was adjusted using the Bonferroni method. Thus, significant eplets were extracted using the significance level set at 0.05 divided by the number of mismatched eplets detected in each cohort.

To compare overall similarities between the β coefficients generated by the Cox proportional hazards model, we calculated weighted Pearson correlation coefficients (r_p) using the “wtd.cor()” function of the “weights” R package (version 1.0.4); statistical significance was assessed by testing the null hypothesis that r_p equaled zero using the t -test. Additionally, we examined whether eplets significantly associated with DSA development were biased toward “antibody-verified” eplets. Information on whether a specific eplet is antibody-verified was determined based on the “Antibody Reactivity” column in the HLA Matchmaker Class I/II Reference File (2017.08). A Fisher’s exact test was used to assess whether these eplets were biased toward antibody-verified eplets and those in perfect linkage disequilibrium (JI = 1.0) with them.

We assigned weights to each mismatched eplet by taking the inverse of the sum of its JIs with other mismatched eplets. Complex associations between mismatched eplets can bias correlation results, and eplets that are frequently detected as mismatched eplets along with other eplets have too large an impact on the correlation results. Therefore, we determined weights by calculating the inverse of the sum of JIs with other mismatched eplets.

To aggregate the effect of eplet mismatches on DSA development, a penalized Cox proportional hazards regression model was applied in the derivation cohort (i.e., pediatric living-donor liver transplant cohort), whereby all mismatched eplets were treated as variables using the “survival” (version 3.4.0) and “glmnet” (version 4.1.4) R packages. The tuning parameter λ for the penalization was chosen by 10-fold cross-validation using the “cv.glmnet()” function of the “glmnet” R package (version 4.1.4). The most accurate methodology was selected from the three penalization methodologies (i.e., ridge, lasso, and elastic net); accuracy was based on the HR of the value computed from the tuned model, adjusted for age, gender, and the number of eplet mismatches. Then, the value computed from the best model was termed the “ERS”. To validate the ERS in the validation cohorts, the “survival” R package (version 3.4.0) was used to compute the HR, which was adjusted for age, gender, and the number of eplet mismatches via the Cox proportional hazards model. In the primary analyses, we adjusted for age, gender, and the number of eplet mismatches. As for the sensitivity analyses, we further adjusted for factors known to be associated with DSA development (i.e., acute rejection rate, immunosuppressive protocol, and the number of HLA antigen mismatches) to confirm the robustness of our results. Finally, we developed an ERS focusing solely on antibody-verified eplets and compared its prediction accuracy with that of the original ERS.

We primarily considered the ERS as a continuous variable and used the HR as the primary metric for evaluating its predictive accuracy. However, for visualization purposes, we divided participants in each cohort into three groups using the tertile values of the ERS from the derivation cohort and created Kaplan-Meier plots based on this grouping. For the Kaplan-Meier analysis, statistical significance was evaluated using the log rank (Mantel-Cox) test by implementing the “survdiff()” function of the “survival” R package (version 3.4.0).

In this study, we prioritized deriving the ERS within a cohort characterized by the same organ type and a consistent immunosuppressive protocol—in this case, a single-center, single-department, pediatric living-donor liver transplant cohort. This approach

involved accepting a trade-off in sample size to ensure uniformity in immunosuppressive protocols and surgical procedures. From the planning phase, we recognized through clinical experience that significant differences exist in both the incidence and pattern of DSA development across organ types. We also believed that these differences arise, at least in part, from variations in immunosuppressive protocols and surgical techniques, which are difficult to quantify accurately. Therefore, we believed that including multiple cohorts to increase sample size could risk creating a machine learning model that is influenced by these complex, difficult-to-quantify factors. By focusing on a single cohort where patients were treated by the same team at the same institution, we thought that we were able to ensure a relatively uniform immunosuppressive protocol and consistent surgical procedures. Therefore, we believed that deriving the ERS in this single-center, single-department, single-organ cohort—specifically a pediatric liver transplant cohort due to its higher event rate—would provide a robust foundation for reliable results. Accordingly, we adopted this method in our study design.

However, we believe that, even though it was conducted post-hoc, examining whether the sample size is sufficient to create an accurate predictive model remains informative. For this purpose, we conducted a post-hoc analysis based on the calculation of the sample size required for a precise estimation of the overall outcome probability in the target population, as described by RD Riley et al.³⁷ Briefly, this analysis evaluates the precision of the estimated cumulative outcome incidence confidence intervals using the following equation, where $\hat{\lambda}$ refers to the estimated number of outcome events per person-year, t represents the follow-up duration, and T is the total person-years of follow-up.

$$\left\{ 1 - \exp\left(-\left(\hat{\lambda} + 1.96\sqrt{\frac{\hat{\lambda}}{T}}\right)t\right)\right\} - \left\{ 1 - \exp\left(-\left(\hat{\lambda} - 1.96\sqrt{\frac{\hat{\lambda}}{T}}\right)t\right)\right\}$$

To assess the significance of correlations between the ERS and the MLR results, the “ppcor” R package (version 1.1) was used to calculate ρ_p between the total ERS (DQ-ERS + DR-ERS) and the median percentage of CFSE^{low} T cells in each healthy volunteer pair. The statistical significance was assessed by testing the null hypothesis (i.e., $\rho_p = 0$) using the t -test within the “ppcor” R package (version 1.1). Finally, to assess the effect of anti-eplet antibodies on the percentages of CFSE^{low} T cells in the MLR, we employed the Wilcoxon rank-sum test and compared the value at 0 ng/mL with those at 1×10^2 and 1×10^3 ng/mL.

Throughout the study, whether the data were normally distributed was examined using the Shapiro-wilk test. Based on these results, appropriate statistical methods were selected for the analysis. Two-sided p -values ≤ 0.05 were considered as a measure of statistical significance. Data were presented as medians with IQRs, estimated using 95% CIs or standard error as considered appropriate. Although our plan was to exclude cases with missing data from the analysis, there were no missing values in the data used for the primary analysis. For patients lost to follow-up, we only used the data available up to the point of loss. Statistical analyses were primarily conducted by K.T., who is certified by the Japan Statistical Society (grade2), using self-made R scripts for the statistical R software (version 4.0.5, R Foundation for Statistical Computing). All statistical details of experiments can be found in the figure legends.